

AWARD NUMBER DAMD17-97-1-7211

TITLE: Cell-Cell Adhesion and Insulin-Like Growth Factor I Receptor in Breast Cancer

PRINCIPAL INVESTIGATOR: Marina A. Guvakova

CONTRACTING ORGANIZATION: Thomas Jefferson University
Philadelphia, Pennsylvania 19107

REPORT DATE: September 1998

TYPE OF REPORT: Annual

PREPARED FOR: Commander
U.S. Army Medical Research and Materiel Command
Fort Detrick, Maryland 21702-5012

DISTRIBUTION STATEMENT: Approved for public release; distribution unlimited

The views, opinions and/or findings contained in this report are those of the author(s) and should not be construed as an official Department of the Army position, policy or decision unless so designated by other documentation.

REPORT DOCUMENTATION PAGE

Form Approved
OMB No. 0704-0188

Public reporting burden for this collection of information is estimated to average 1 hour per response, including the time for reviewing instructions, searching existing data sources, gathering and maintaining the data needed, and completing and reviewing the collection of information. Send comments regarding this burden estimate or any other aspect of this collection of information, including suggestions for reducing this burden, to Washington Headquarters Services, Directorate for Information Operations and Reports, 1215 Jefferson Davis Highway, Suite 1204, Arlington, VA 22202-4302, and to the Office of Management and Budget, Paperwork Reduction Project (0704-0188), Washington, DC 20503.

1. AGENCY USE ONLY (Leave blank)		2. REPORT DATE September 1998		3. REPORT TYPE AND DATES COVERED Annual (15 Aug 97 - 14 Aug 98)	
4. TITLE AND SUBTITLE Cell-Cell Adhesion and Insulin-Like Growth Factor I Receptor in Breast Cancer				5. FUNDING NUMBERS DAMD17-97-1-7211	
6. AUTHOR(S) Marina A. Guvakova					
7. PERFORMING ORGANIZATION NAME(S) AND ADDRESS(ES) Thomas Jefferson University Philadelphia, Pennsylvania 19107				8. PERFORMING ORGANIZATION REPORT NUMBER	
9. SPONSORING / MONITORING AGENCY NAME(S) AND ADDRESS(ES) U.S. Army Medical Research And Materiel Command ATTN: MCMR-RMI-S 504 Scott Street Fort Detrick, Maryland 21702-5012				10. SPONSORING / MONITORING AGENCY REPORT NUMBER	
11. SUPPLEMENTARY NOTES					
12a. DISTRIBUTION / AVAILABILITY STATEMENT Approved for public release; distribution unlimited				12b. DISTRIBUTION CODE	
13. ABSTRACT (Maximum 200 words) Disorganized epithelial tissue morphology is a prerequisite of breast tumor progression. Determining the mechanisms controlling cell-cell interactions will be a step towards the understanding how to prevent processes of tumor cell spreading, invasion and metastasis. Accumulating evidence suggests an important role of a natural modulator, such as insulin-like growth factor (IGF-I), and the pharmacological compounds, including antiestrogens, in regulating of E-cadherin-mediated intercellular adhesion in breast carcinomas. Molecular mechanisms, by which IGF-I and antiestrogens modulate cell-cell associations, have not been clarified. In the present work, we investigated the functional role of different IGF-I receptor (IGF-IR) domains in E-cadherin-mediated intercellular aggregation. The major achievement of this work is the development of the unique model consisting of MCF-7-derived human breast cancer cells, in which the normal IGF-IR is partially or completely inactivated by co-expression of its dominant-negative forms. Taking advantage of this model, we determined that IGF-IR catalytic activity and signaling mediated by the C-terminal region of the IGF-IR are critical for aggregation of MCF-7 breast cancer cells grown on the extracellular matrix. Additionally, we discovered that in MCF-7 cells, a non-steroidal antiestrogen Tamoxifen inhibited cell growth in monolayer and in three-dimensional culture, which was associated with blocked IGF-IR/IRS-1-mediated signaling.					
14. SUBJECT TERMS Breast Cancer				15. NUMBER OF PAGES 60	
				16. PRICE CODE	
17. SECURITY CLASSIFICATION OF REPORT Unclassified	18. SECURITY CLASSIFICATION OF THIS PAGE Unclassified	19. SECURITY CLASSIFICATION OF ABSTRACT Unclassified	20. LIMITATION OF ABSTRACT Unlimited		

FOREWORD

Opinions, interpretations, conclusions and recommendations are those of the author and are not necessarily endorsed by the U.S. Army.

N/A Where copyrighted material is quoted, permission has been obtained to use such material.

N/A Where material from documents designated for limited distribution is quoted, permission has been obtained to use the material.

M.G. Citations of commercial organizations and trade names in this report do not constitute an official Department of Army endorsement or approval of the products or services of these organizations.

N/A In conducting research using animals, the investigator(s) adhered to the "Guide for the Care and Use of Laboratory Animals," prepared by the Committee on Care and use of Laboratory Animals of the Institute of Laboratory Resources, national Research Council (NIH Publication No. 86-23, Revised 1985).

M.G. For the protection of human subjects, the investigator(s) adhered to policies of applicable Federal Law 45 CFR 46.

M.G. In conducting research utilizing recombinant DNA technology, the investigator(s) adhered to current guidelines promulgated by the National Institutes of Health.

M.G. In the conduct of research utilizing recombinant DNA, the investigator(s) adhered to the NIH Guidelines for Research Involving Recombinant DNA Molecules.

M.G. In the conduct of research involving hazardous organisms, the investigator(s) adhered to the CDC-NIH Guide for Biosafety in Microbiological and Biomedical Laboratories.


PI - Signature 9/3/98
Date

TABLE OF CONTENTS

	Page
Front Cover	1
Report Documentation Page	2
Foreword	3
Table of Contents	4
Introduction	5
Body/Technical Report	7
Conclusions	18
References	19
Appendix	20

INTRODUCTION

The most advanced steps of breast cancer progression, such as cell invasion and metastasis, are accompanied by disruption of epithelial tissue integrity (1). The substantial evidences exist that a malfunction of the zonula adherence junctions leads to enhancement of cell invasiveness in vitro and metastasis of certain human tumors (2, 3). In epithelial cells, the transmembrane glycoprotein E-cadherin, which is localized to adherens junctions where it is associated with the cytoplasmic proteins of the catenin family, exhibits the major adhesion activity (4). Although the mechanism controlling the activation of E-cadherin is not well understood, the modulatory role of extracellular stimuli including different growth factors was strongly suggested (5-9).

In human breast cancer cells, insulin-like growth factor I (IGF-I), acting through the specific receptor (IGF-IR) was shown to inhibit invasiveness, presumably via stimulation of E-cadherin-mediated adhesion (10). Additionally, non-steroidal antiestrogen Tamoxifen was implicated in the up-regulation of cell aggregation in vitro, thereby suggesting the potential function of antiestrogens as anti-scattering agents (11). Despite these intriguing findings, it remains unexplored how IGF-IR stimulation leads to up-regulation of the adherens type cell junctions and whether antiestrogens favor this process.

The **purpose** of our study is to elucidate molecular mechanisms by which IGF-IR and antiestrogens modulate cell-cell adhesion in breast carcinomas. We believe that the understanding of the mechanisms governing epithelial cell adhesiveness is a crucial and necessary step in the design and development of therapeutic approaches against invasive and, consequently, the most aggressive breast carcinomas.

Realizing the complex nature of the investigated phenomenon, we addressed the following discrete **questions**: 1) How IGF-IR regulates adherens junctions? 2) Which elements of the E-cadherin complex are critical for IGF-I-stimulated adhesion? 3) Do antiestrogens stimulate cell-cell adhesion through modification of adherens molecules and /or IGF-IR signaling pathways?

In order to answer the above questions, our experimental work is guided by the **specific aims:**

- 1. To determine whether the intact IGF-IR signaling is critical for the activation of cell-cell adhesion in breast cancer cells.** To approach, this aim, we proposed to pursue the comparative analysis of the aggregation in the cells expressing the functional versus inactive/partially active IGF-IR. In our preliminary work, we have generated clones of MCF-7 breast cancer cells overexpressing the wild type IGF-IR and revealed their enhanced ability to aggregate on the extracellular matrix (12). This project is further directed towards the development of MCF-7 clones overexpressing inactive or partially active IGF-I receptors, in which IGF-IR signaling and ability to grow in aggregates will be characterized.
- 2. To identify the protein/s of the E-cadherin adhesion complex, which are necessary for IGF-I-induced cell aggregation in breast epithelia.** As we have shown, the wild type IGF-IR is co-localized with E-cadherin into cell-cell junctions in the poorly invasive MCF-7 cells (12). Furthermore, we and others have discovered physical association of the IGF-IR signaling molecules with the elements comprising the cadherin complex (12, 13, 14). Using the invasive breast cancer cell lines defective in the expression of either E-cadherin or catenins, we further intend to distinguish which of these adhesion molecule/s are indispensable for IGF-I-promoted cell aggregation.
- 3. To explore the potential of antiestrogens in upregulating of cell aggregation.** As reported before, Tamoxifen restored the function of E-cadherin in invasive breast cancer cells in vitro via unknown mechanism (11). Our aim is to investigate the influence of nonsteroidal antiestrogen Tamoxifen and of a pure antiestrogen ICI 182, 780 on the aggregation of breast cancer cells. We also plan to test possible effects of these antiestrogens on IGF-IR signaling molecules and the proteins comprising the E-cadherin complex.

TECHNICAL REPORT

PI dedicated 100% of her working time to this project and, in accordance with the proposed Statement of Work, obtained the following results relevant to:

AIM 1. To explore a functional role of IGF-IR signaling in breast cancer cell aggregation, I developed and characterized clones of MCF-7 human breast cancer cells overexpressing different mutant IGF-IRs with inactivated signaling.

Part I: *Development of the mutant clones.*

The clones of MCF-7 cells expressing mutant IGF-I receptors were generated by stable transfection (12) with the pcDNA3 expression vector containing the following human IGF-IR cDNAs:

- The IGF-R cDNA, encoding the IGF-IR, in which C-terminus was truncated at the position 1229, right below the tyrosine kinase domain, referred as **TC** (15). This cDNA, cloned in pcDNA3, was obtained from Dr. E. Surmacz.
- The IGF-IR cDNA, encoding the IGF-IR, in which the cluster of three tyrosine residues in the kinase domain (at positions 1131,1135,1136) was replaced by phenylalanine residues, referred as **YF3** (16), and
- The IGF-IR cDNA encoding the IGF-IR with a substitution of lysine in the ATP binding site (position 1003) by arginine, referred as **KR** (17). Both cDNAs, cloned in pBluscript II KS+, were generously provided by Dr. D. LeRoith (NIH).

The last two mutant cDNAs were excised from the pBluscript II KS+ vector with EcoRI and XbaI restriction enzymes and cloned under the CMV promoter into the pcDNA3 expression vector encoding a neomycin resistance gene (Invitrogen). The cloning of inserts was verified by restriction digestion, and the new vectors were transfected into MCF-7 cell. The antibiotic-resistant clones were selected in culture medium containing 1 mg/ml G418 (Geneticin) (Gibco BRL). The incorporation of the TC mutant cDNA into genome was analyzed by PCR (polymerase chain reaction) as described in details in our previous work (12). To compare the level of the IGF-IR in antibiotic-resistant clones,

fluorescence-activated cell sorting (FACS) analysis was performed in all types of the mutant clones (FACS assay is described in details in Ref. 12).

Type of IGF-IR cDNA transfected into MCF-7 cells	TC	YF3	KR
Number of transfected MCF-7 cells ($\times 10^6$)	4.6	2.0	2.0
Number of isolated Neomycin-resistant colonies	66	69	53
Number of PCR-positive clones/tested	9/55	N/A	N/A
Number of FACS-positive clones/tested	6/49	13/38	11/19

Table 1. Development of MCF-7 cell clones expressing different mutants of the IGF-IR. Summarized data are presented on the efficiency of MCF-7 cell transfection and selection. N/A, data are not available.

In some samples of the antibiotic-resistant TC transfectants, PCR analysis was found to give a false negative result. In these cells, the incorporation of the cDNA insert could not be detected, despite the evident IGF-IR protein overexpression proved by the other techniques (FACS and Western blotting). For this reason, in the following screening of YF3 and KR transfectants, PCR test was omitted and FACS analysis was performed instead. This latter test was found to be more reliable and informative, as it is identifying the positive clones and estimating the level of IGF-IR expression on the cell surface.

Thus, the applied strategies resulted in a successful generation of the unique collection of MCF-7 breast cancer epithelial cells overexpressing the mutant, presumably dominant negative, forms of the IGF-IR.

Part II: Evaluation of IGF-IR number in the mutant clones.

From the groups of FACS-positive MCF-7 clones, the clones with the maximal fluorescence of the IGF-IR were chosen and designated as:

MCF-7, TC, – with truncated C-terminus,

MCF-7, YF3, -- with mutated kinase domain,

MCF-7, KR, -- with inactive ATP-binding site.

The clones overexpressing the wild type IGF-IR and the ones transfected with control pcDNA3 plasmid are referred as **MCF-7, WT** and **MCF-7, NEO**, respectively.

To compare IGF-IR level in clones overexpressing the wild type and mutant receptors, FACS analysis was performed using an anti-IGF-IR monoclonal antibody (IGF-IR mAb) (Oncogene Science) (Fig.1). The approximate number of the IGF-IR per cell was estimated as a function of the relative fluorescence (Table 2).

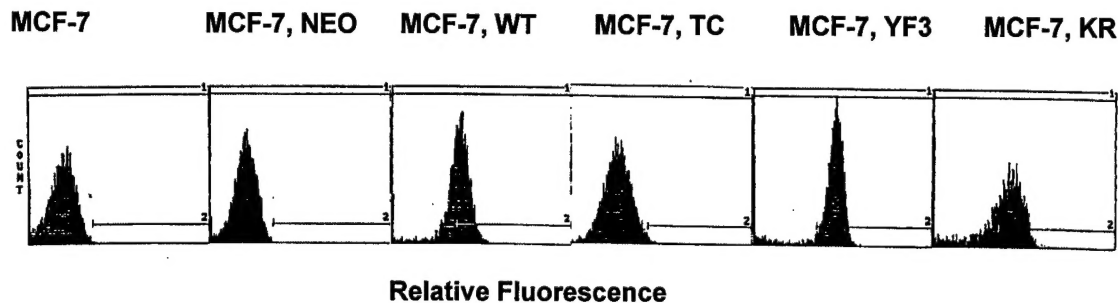


Fig. 1. Comparative analysis of the MCF-7-derived clones expressing the wild type and mutant IGF-IRs. Abscissa: Relative fluorescence; ordinate: Cell number. The representative results of two experiments are shown.

Cell type	MCF-7	MCF-7, NEO	MCF-7, WT	MCF-7, TC	MCF-7, YF3	MCF-7, KR
K_{FACS}	1.0	1.0	4.8	2.3	7.8	4.7
IGF-IR/cell ($\times 10^6$)	0.06	0.06	1.10	~0.13	~1.80	~1.00

Table 2. Estimation of the IGF-IR level in MCF-7 cell transfectants. K_{FACS} represents a ratio of the relative fluorescence mean in a population of 5×10^3 of transfectants to that parameter in MCF-7 cells. ~, The number of the IGF-IR is approximated proportionally to K_{FACS} .

FACS analysis, based on a highly specific interaction of an anti-IGF-IR antibody and the specific IGF-IR, was performed instead of Scatchard analysis. Since the latter may overestimate the levels of receptor as it determines the number of total ligand binding sites, including those of high affinity representing IGF-IRs and those of low affinity representing IGF-I binding proteins. The additional advantages of FACS analysis are that it is relatively quick, inexpensive and does not involve the usage of radioactive materials.

Therefore, the applied approach facilitated characterization of IGF-IR level in the mutant MCF-7 clones.

Part III: Characterization of IGF-IR signaling in the mutant clones.

The IGF-IR is a receptor type tyrosine kinase, in which autophosphorylation of the transmembrane beta subunit is increased upon binding of IGF-I. Being activated, the IGF-IR recruits and phosphorylates several substrates. Among them, the major substrates are insulin receptor substrate 1 (IRS-1) and src-homology/collagen proteins (SHC, p46 and p52). When tyrosine phosphorylated, IRS-1 molecules attract multiple signaling proteins including the regulatory subunit of phosphatidylinositol 3 (PI3)-kinase (p85) and the adaptor molecules such as Grb2, Crk, Nck that constitute the scaffold of the IGF-IR signal transduction cascade. Tyrosine phosphorylated SHC proteins also bind to Grb2. Most of the adaptor molecules stimulate the mitogen-activated protein (MAP) kinase pathway. In particular, induction of the IGF-IR signaling cascade results to rapid activation of Erk1 and Erk2 kinases, which are implicated in mitogenesis.

To identify which of IGF-IR signaling pathways are impaired or blocked in MCF-7 mutant clones, the activity of the best known elements of the IGF-IR signaling cascade were investigated (Fig. 2). The level of IGF-I-induced tyrosine phosphorylation of the IGF-IR and its two major substrates, IRS-1 and SHC was measured by Western blotting. Briefly, subconfluent cells were serum starved for 24 hours, then incubated in either serum-free medium (SFM) alone or SFM supplemented with 50 ng/ml IGF-I for 5 minutes. Cell lysates containing 300 µg of the total protein were incubated with one of the following antibodies: an anti-IGF-IR mAb (Oncogene Science), an anti-IRS-1 pAb (UBI), or an anti-SHC pAb (Transduction Laboratories). The precipitated proteins were resolved by PAGE, transferred onto the nitrocellulose filter, and hybridized with an anti-phosphotyrosine antibody (Santa Cruz). The amount of the precipitated proteins was measured in the anti-phosphotyrosine blots after stripping and re-probing with either an anti-IGF-IR β pAb (Santa Cruz), an anti-IRS-1 pAb (UBI), or an anti-SHC mAb (Santa Cruz).

To study the activation of the PI3-kinase signaling, which is one of the downstream IGF-IR/IRS-1-mediated pathways, the interaction between the PI3-kinase regulatory subunit (p85) and IRS-1 was analyzed. In parallel experiments, the association of the adaptor molecule Grb2 and SHC, known to promote Ras/MAP kinase

mitogenic cascade was examined. The protein levels of IRS-1- and SHC-associated molecules were determined after stripping of IRS-1 and SHC blots and re-probing with an anti-PI3-kinase (p85) pAb (UBI) and an anti-Grb2 mAb (Transduction Laboratories), respectively.

The activity of MAP kinases (Erk1 and Erk2) was assessed in the whole lysates by immunoblotting with an anti-active MAPK antibody (Promega). The protein levels of MAP kinases were detected in the same blots after stripping and re-probing with an anti-Erk1 pAb (Santa Cruz).

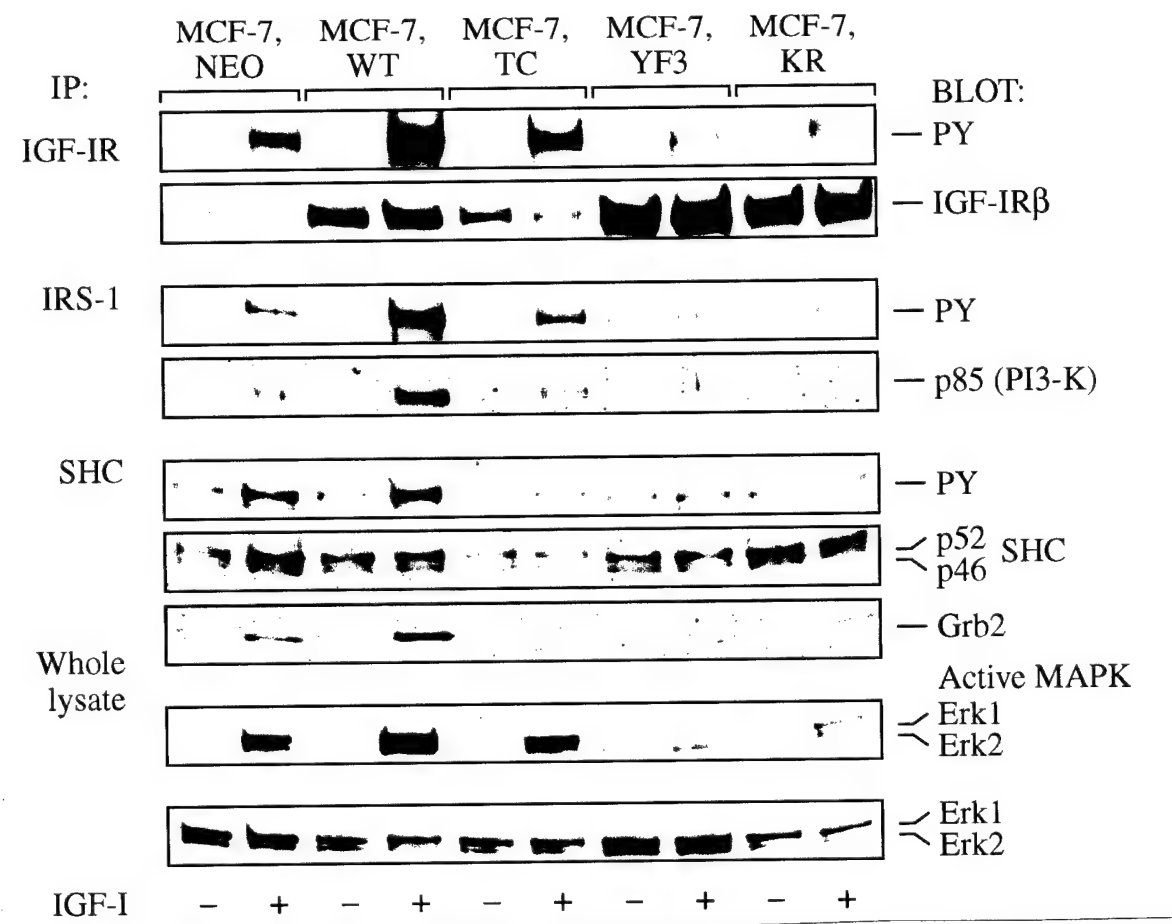


Fig. 2. IGF-IR signaling in the mutant clones. The summarized data on the activity of the IGF-IR signaling molecules are shown. Each panel is representative of two separate experiments. Protein level of IRS-1 was similar in all transfectants. The corresponding blot is not shown because it has a heavy background. Anti-Erk1 pAb recognized both Erk1 and Erk2 proteins.

The IGF-IR protein level in **MCF-7,TC** precipitates was slightly higher than that found in **MCF-7,NEO** cells, which corresponded with the results of FACS analysis. In these mutant cells, IGF-I-induced tyrosine phosphorylation of the IGF-IR and IRS-1 as well as

the amount of IRS-1-associated PI3-kinase resembled the correspondent levels in MCF-7,NEO cells. In contrast, tyrosine phosphorylation of SHC was not induced in response to IGF-I, and Grb2 binding to SHC was barely detectable, suggesting at least partial block of SHC-activated pathway/s in MCF-7,TC cells.

In **MCF-7,KR** precipitates, the amount of the IGF-IR protein was found to be similar to that seen in MCF-7,WT cells , however, IGF-I-induced tyrosine phosphorylation of the IGF-IR β -subunit, IRS-1 and SHC was lower than that in cells overexpressing the wild type IGF-IR. These results suggest that in MCF-7,KR mutants, IRS-1/PI3-kinase-dependent signaling is significantly reduced (it is lower than in the parental MCF-7 cells) and SHC/Grb2 function is considerably blocked.

MCF-7,YF3 mutants expressed almost twice as much of the IGF-IR protein than MCF-7,WT cells. It is most likely that due to the extremely high dominant-negative receptor expression the kinase activity of the endogenous IGF-IR was completely blocked in MCF-7,YF3 cells. Indeed, IGF-I stimulation increased neither IGF-IR autophosphorylation nor phosphorylation of the receptor substrates.

IGF-I-promoted MAP kinase activity was reduced in MCF-7,KR mutant cells compare to MCF-7,WT cells. Activation of MAP kinases by IGF-I was completely abrogated in **MCF-7,YF3** cells. Interestingly, in these cells the basal Erk2 but not Erk1 kinase was moderately activated and sustained at this level even after IGF-I stimulation. In **MCF-7,TC** mutants the extent of MAPK activation was indistinguishable from that seen in control MCF-7,NEO cells.

Part IV: Aggregation of the mutant clones.

The aggregation of the clones expressing different mutant IGF-IRs was compared with that in cells expressing the similar amount of the wild type IGF-IR. Cells were tested in Matrigel outgrowth assay where cells grew on the top of extracellular matrix (ECM) consisting of the major basement membrane components. This assay represents a closest in vitro model for tumor growth in vivo. Briefly, a cell suspension was plated on Matrigel (Biocoat) into 24-well plates (2×10^4 cells/well). The cells were maintained in a regular culture medium (DMEM/F12) supplemented with 5% of calf serum. On day 14 after plating, the amount of aggregates of the certain size was directly counted under the microscope with an ocular ruler (Table 3). The morphology of aggregates was photographed at day 21 (Fig. 3).

Cell type	MCF-7, NEO	MCF-7, WT	MCF-7, TC	MCF-7, YF3	MCF-7, KR
Number of aggregates/ well, size $\geq 150 \mu\text{m}$	109	182	86	150	101
Number of aggregates/ well, size $\geq 300 \mu\text{m}$	79	111	3	34	2

Table 3. Measurement of size and amount of aggregates in MCF-7 cells overexpressing different mutant IGF-IRs. The average of two independent experiments with duplicates is presented.

The cells overexpressing the wild type IGF-IR being plated on Matrigel formed generally more aggregates and of the bigger sizes then the parental cells. The increased expression of the mutant IGF-IRs in MCF-7 cells resulted to the essential reduction in the amount of aggregates especially of a size $\geq 300 \mu\text{m}$: 96%, 70%, 98% inhibition was observed in TC, YF3 and KR clones of MCF-7 cells, respectively.

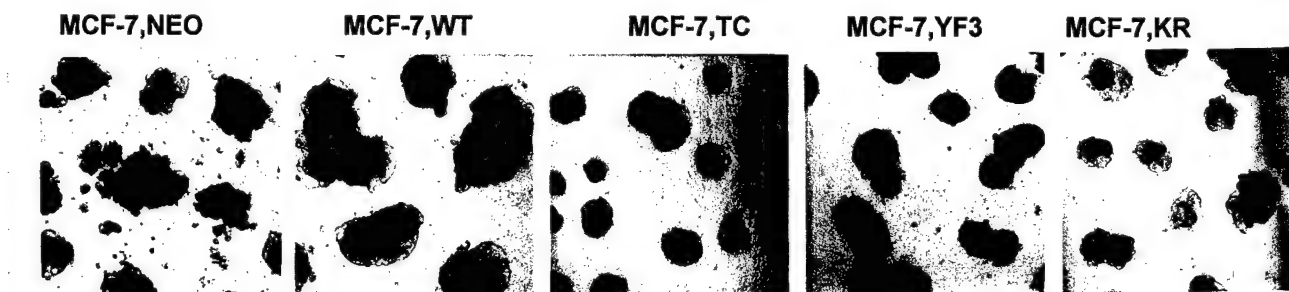


Fig. 3. Morphology of aggregates of MCF-7 cells overexpressing the mutant IGF-IRs. Representative phase-contrast micrographs are shown. Scale bar, $150 \mu\text{m}$.

Therefore, MCF-7 cells overexpressing the mutant IGF-IR with inactivated kinase function were less capable of forming/supporting aggregates. These data strongly point to the conclusion that IGF-IR catalytic activity is crucial for development of aggregates by cells grown on extracellular matrix. In addition, the C-terminal domain is necessary to stimulate cell-cell adhesion.

Part V: Analysis of IGF-IR/E-cadherin association in the mutant clones.

In MCF-7 cells expressing the wild type IGF-IR, E-cadherin and its associated proteins from the catenin family were found in IGF-IR precipitates (12). Furthermore, in cells overexpressing the IGF-IR, greater amounts of this receptor associated with E-cadherin relatively to the parental cells (13). In order to analyze whether the mutant IGF-IRs interact with adhesion molecules, the amount of E-cadherin and β -catenin was measured in IGF-IR precipitates of MCF-7 mutants (Fig. 4).

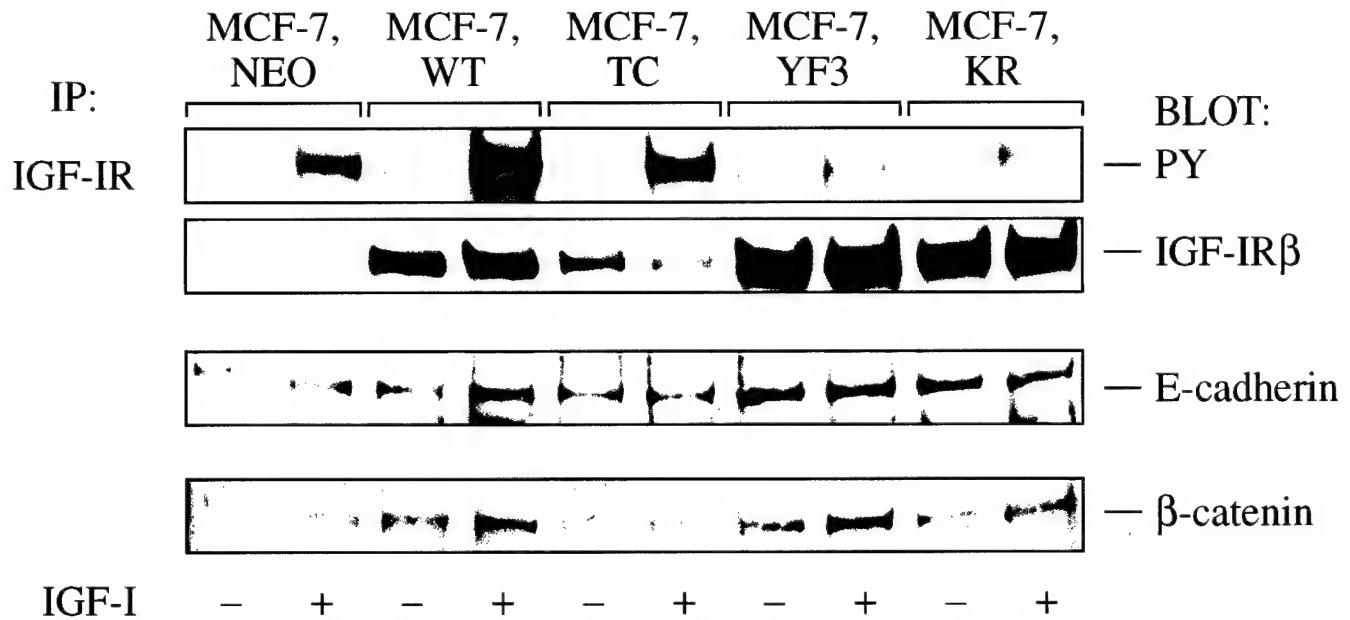


Fig. 4. Association of the mutant IGF-IRs with E-cadherin/ β -catenin. The IGF-IR tyrosine phosphorylation and protein level was measured by immunoblotting with anti-phosphotyrosine and anti-IGF-IR β antibodies, respectively.

Briefly, serum-starved cells were treated with 50 ng/ml IGF-I for 5 minutes and lysed. The IGF-IR was precipitated with an anti-IGF-IR mAb (Oncogene Science) from 300 μ g of protein from unstimulated and IGF-I-stimulated cells. The amount of co-precipitated E-cadherin and β -catenin was assessed by Western blotting with an anti-E-cadherin mAb (Transduction Laboratories) and β -catenin anti-serum (Sigma), respectively.

As expected, the increased amounts of E-cadherin and β -catenin were co-precipitated with the IGF-IR in MCF-7, WT relatively to the control MCF-7, NEO cells. Interestingly, in cells overexpressing the mutant forms of the IGF-IR, the considerably increased amounts of the adhesion molecules were also found in IGF-IR precipitates.

Therefore, the alterations in the IGF-IR, at least the mutations and truncation studied here, appeared not to block the IGF-IR/E-cadherin association. Additionally, this interaction seemed to be independent on the tyrosine phosphorylation status of the IGF-IR. Possibly, protein modifications other than phosphorylation on tyrosine residues are of critical importance for the maintenance of the interaction between the IGF-IR and E-cadherin complexes. Further analysis should also clarify whether α -catenin, the protein coupling the adherence molecules to the actin cytoskeleton, is associated with the mutant IGF-IRs.

AIM 3. To explore the role of antiestrogens in cell aggregation, I investigated the effect of a non-steroidal antiestrogen Tamoxifen on IGF-IR-mediated functions.

Part I. *Effect of Tamoxifen on cell aggregates.*

To evaluate the potential influence of Tamoxifen on cell aggregation and growth in aggregates, the three-dimensional cultures of MCF-7 and MCF-7 cells overexpressing the wild type IGF-IR (50-times increase) were exposed to a prolonged Tamoxifen treatment. Briefly, a cell suspension of 2×10^4 cells in culture medium was plated into 24-well plates coated with the extracellular matrix (Matrigel). After 5 days, the medium was substituted by SFM (control) and SFM containing either 50 ng/ml IGF-I or 10 nM Tamoxifen. Cells were photographed after one week of treatment (Fig.5).

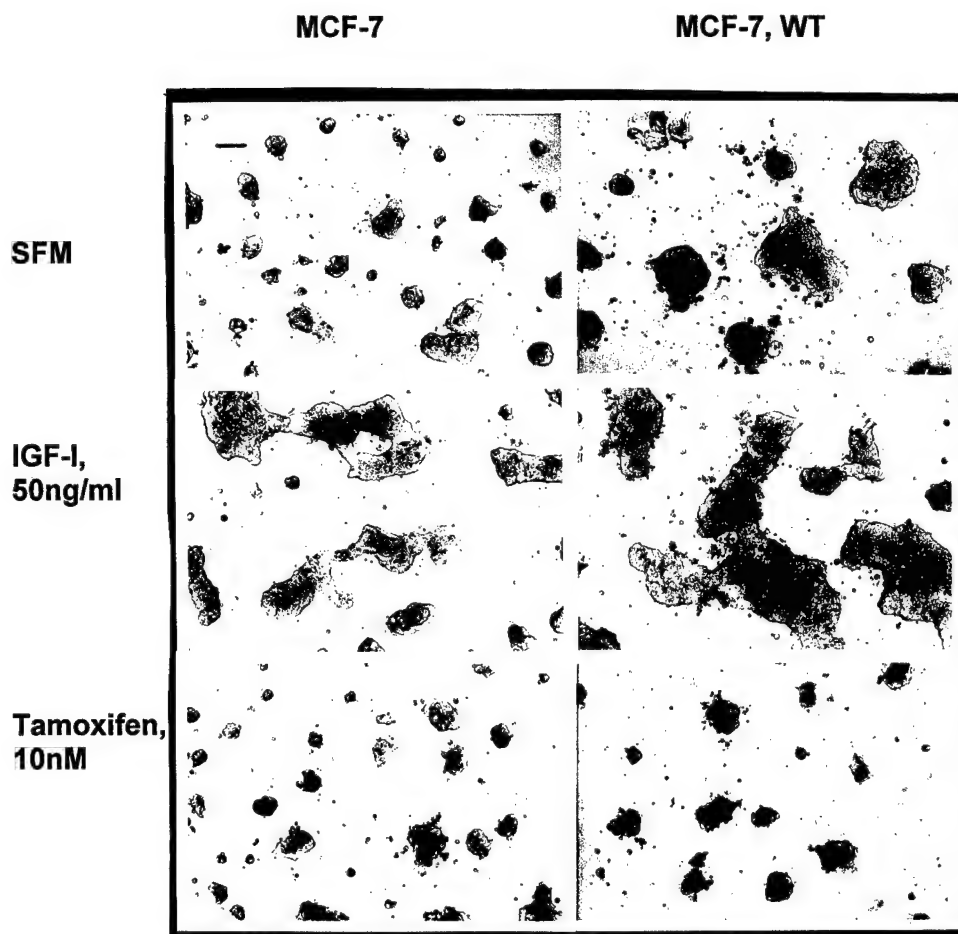


Fig. 5 The representative morphology of the aggregates grown on Matrigel and treated with either IGF-I or Tamoxifen for 7 days. Scale bar, 100 μ m.

In these experiments IGF-I promoted the appearance of huge aggregates, whose sizes were technically difficult to measure because of their irregular shape. In contrast, Tamoxifen treatment, especially of MCF-7 cells with amplified IGF-IR, caused the prominent reduction of aggregate sizes from 250-300 μ m (in control cells in SFM) to 80-100 μ m (in Tamoxifen-treated cells) on the average. Thus, unexpectedly, in non-invasive MCF-7 breast cancer cells, Tamoxifen did not improve the aggregation but rather reduced growth and/or survival of cells grown on Matrigel.

Part II. Effect of Tamoxifen on cell growth in monolayer.

To test growth inhibitory effect of Tamoxifen on the cells with amplified IGF-IR signaling, the monolayer growth of MCF-7 and MCF-7,WT cells (with 8-and 50-fold overexpression) was examined in the presence of Tamoxifen. Subconfluent cells were treated with Tamoxifen for 4 days (see Ref. 18 for technical details). Dose-dependence assay with a range of drug concentration 0.1-100 nM revealed that 10 nM Tamoxifen suppressed the growth of all tested cell lines by 45-60%, regardless the level of IGF-IR magnification (see Fig. 1 in Ref. 18).

Part III. Effect of Tamoxifen on IGF-IR signaling.

The potential influence of Tamoxifen on the intercellular IGF-IR signaling was investigated in the cells whose growth in monolayer was reduced by subtoxic dose of Tamoxifen (10 nM). The growth inhibitory activity of Tamoxifen was accompanied by downregulation of IGF-I-induced tyrosine phosphorylation of the IGF-IR and inhibition of basal and IGF-I-induced tyrosine phosphorylation of IRS-1 molecules. Moreover, Tamoxifen reduced IRS-1-associated PI3-kinase activity, at least partially due to a decreased binding of the regulatory subunit (p85) to IRS-1. Interestingly, in Tamoxifen-treated cells, Grb2 association with IRS-1 was notably reduced, while association of Grb 2 with another IGF-IR substrate SHC was considerably enhanced (detailed results are presented in Ref. 18).

Part IV. Effect of a pure antiestrogen ICI 182,780 on IGF-IR signal transduction.

In a collaborative work with the Department of Cellular Biology at the University of Calabria, Italy, we have begun the study on the effect of a pure antiestrogen ICI 182,780 on IGF-IR signaling. We have shown that this drug in a dose-dependent manner inhibited the basal and IGF-I-induced growth of MCF-7 clones overexpressing the IGF-IR, IRS-1 and SHC. Remarkably, the overexpression of IRS-1 molecule endowed the cells with the enhanced resistance to ICI 182,780 cytostatic effect. By Northern and Western blotting, it was shown that antiestrogen ICI 182,780 reduced IRS-1 protein expression and tyrosine phosphorylation, which in turn resulted in decreased binding of p85 (PI3-kinase) and Grb2 to IRS-1 (see submitted manuscript in appendix).

CONCLUSIONS

The elucidation of the regulatory mechanisms governing cell-cell adhesion and three-dimensional growth are of a great importance for understanding and controlling the processes of tumor cell spreading and metastasis. The purpose of the presented work was to evaluate the functional role of IGF-IR signaling and the potential effect of antiestrogens on breast cancer cell aggregation. Summing up the results, the following conclusions can be drawn:

- **In this study, the unique model consisting of MCF-7 human breast cancer cells overexpressing a partially or totally inactivated IGF-IR was developed and characterized.**
- **The comparative analysis of breast cancer cells overexpressing the wild and mutant forms of IGF-IR demonstrated the critical importance of IGF-IR signaling in the development of the multicellular aggregates.**
- **For the first time, it was established that the IGF-IR tyrosine kinase contributed into regulation of breast cancer cell aggregation in three-dimensional culture.**
- **Additionally, this study revealed that the activation of the functional kinase domain as well as the C-terminal region of the IGF-IR played a regulatory role in aggregation of breast cancer cells.**
- **In non-invasive breast cancer cells, antiestrogen Tamoxifen was found to diminish IGF-IR/IRS-1 signaling, inhibit cell growth in monolayer, and reduce the size of tumor cell aggregates in vitro.**

The generated MCF-7 cells overexpressing the wild and mutant types of IGF-IR will certainly serve as a valuable model for the further studies on the mechanisms of IGF-IR-regulated cell aggregation in breast cancer cells.

Indeed, cell aggregation itself is a complex and multistep process. Firstly, cells plated on Matrigel interact with the elements of the ECM, secondly, they develop locomotive reactions, which allow them to crawl over substratum, then contact each other via cell junctions, aggregate and, eventually, grow as a three-dimensional culture. Our future investigations should clarify, which of those intermediate steps of cell aggregation are affected by IGF-IR signaling in breast cancer cells.

PAPERS (published and submitted)

1. Guvakova M. A., Surmacz E. Overexpressed IGF-I receptors reduce estrogen growth requirement, enhance survival and promote E-cadherin-mediated cell-cell adhesion in human breast cancer cells. *Exp. Cell Res.* 231:149-162, 1997.
2. Guvakova M. A., Surmacz E. Tamoxifen interferes with the insulin-like growth factor I receptor (IGF-IR) signaling pathways in breast cancer cells. *Cancer Research*, 57:2606-2610, 1997.
3. Surmacz E., Guvakova M. A., Nolan M. K., Nicosia R. F., Sciacca L., Type I insulin-like growth factor receptor function in breast cancer, *Breast Cancer Research and Treatment*, 47: 255-267, 1998.
4. Salerno M., Sisci D., Mauro L., Guvakova M. A., Ando S., Surmacz E. Insulin-receptor substrate 1 (IRS-1) is a target for pure antiestrogen ICI 182, 780 in breast cancer cells. (Submitted).

REFERENCES:

1. M. Takeichi, *Current Opin. Cell Biol.* **5**, 806 (1993).
2. K. Pantel et al., In: *Cell adhesion and human disease*. Wiley, Chichester (Ciba Foundation Symposium 189), 157 (1995).
3. W. Zschiesche et al., *Anticancer Res.* **17(1B)**, 561 (1997).
4. Y. Shimoyama et al., *Cancer Res.*, **49**, 2128 (1989).
5. M. Ozawa et al., *Proc. Natl. Acad. Sci. USA* **87**, 4246 (1990).
6. W. Birchmeier et al., In: *Cell adhesion and human disease*. Wiley, Chichester (Ciba Foundation Symposium 189), 124 (1995).
7. P. J. Miettinen et al., *J. Cell Biol.* **127**, 2021 (1994).
8. B. D'Souza and J. Taylor-Papadimitriou, *Proc. Natl. Acad. Sci. USA* **91**, 72-2 (1994).
9. H. Hoscheuetzky et al., *J. Cell Biol.* **127**, 1375 (1994).
10. S. Shibamoto et al., *Cell Adhesion and Communication* **1**, 295 (1994).
11. M. E. Bracke et al., *Cancer Res.* **54**, 4607 (1994).
12. M. A. Guvakova and E. Surmacz, *Exp. Cell Res.* **231**, 149 (1997).
13. E. Surmacz et al., *Breast Cancer Res. Treat.* **47**, 255 (1998).
14. Y. Xu et al., *J. B. C.* **272**, 13463 (1997).
15. E. Surmacz et al., *Exp. Cell Res.* **218**, 370 (1995).
16. H. Kato et al., *Mol. Endocrinology* **8**, 40 (1994).
17. H. Kato et al., *J. B. C.*, **268**: 2655 (1993).
18. M. A. Guvakova and E. Surmacz, *Cancer Res.* **57**, 2606 (1997)

APPENDIX

Papers:

1. Guvakova M. A., Surmacz E. Overexpressed IGF-I receptors reduce estrogen growth requirement, enhance survival and promote E-cadherin-mediated cell-cell adhesion in human breast cancer cells. *Exp. Cell Res.* 231:149-162, 1997 (**Ref. 12**).
2. Guvakova M. A., Surmacz E. Tamoxifen interferes with the insulin-like growth factor I receptor (IGF-IR) signaling pathways in breast cancer cells. *Cancer Research*, 57:2606-2610, 1997 (**Ref. 18**).
3. Salerno M., Sisci D., Mauro L., Guvakova M. A., Ando S., Surmacz E. Insulin-receptor substrate 1 (IRS-1) is a target for pure antiestrogen ICI 182, 780 in breast cancer cells. (**Submitted**).

Overexpressed IGF-I Receptors Reduce Estrogen Growth Requirements, Enhance Survival, and Promote E-Cadherin-Mediated Cell–Cell Adhesion in Human Breast Cancer Cells

MARINA A. GUVAKOVA AND EWA SURMACZ¹

Kimmel Cancer Institute, Thomas Jefferson University, Philadelphia, Pennsylvania 19107

INTRODUCTION

The insulin-like growth factor I receptor (IGF-IR) paracrine or autocrine loop plays an important role in the maintenance of breast cancer growth. Cancer cells contain several-fold higher levels of the IGF-IR than normal breast tissue; however, it is still not clear whether abnormally high activation of IGF-IR signaling may induce progression of the disease. To address this question, we have established several MCF-7-derived clones (MCF-7/IGF-IR cells) overexpressing the IGF-IR. We report here that overexpression of the IGF-IR did not modify sensitivity of cells to IGF-I; however, responsiveness to the ligand was moderately enhanced in most of the MCF-7/IGF-IR clones (measured by [³H]-thymidine incorporation into DNA). All MCF-7/IGF-IR clones responded to the synergistic action of 1 nM estradiol (E2) and small amounts of IGF-I (up to 0.8 ng/ml). Exposure of cells to higher concentrations of IGF-I abolished estrogen requirements for stimulation of DNA synthesis in all MCF-7/IGF-IR clones, but not in the parental cells. The most important finding of this work was that the amplification of the IGF-IR induced cell–cell adhesion in MCF-7 cells. High levels of the IGF-IR promoted cell aggregation on Matrigel, allowed proliferation of cells within the aggregates, and protected clustered cells from death. In both MCF-7 and MCF-7/IGF-IR cells, IGF-I stimulated aggregation, whereas an anti-E cadherin antibody blocked cell–cell adhesion. Furthermore, immunofluorescence staining with specific antibodies revealed co-localization of the IGF-IR and E-cadherin at the points of cell–cell contacts. Moreover, the IGF-IR and its two substrates, insulin receptor substrate 1 and SHC, were contained within the E-cadherin complexes. Our results suggest that overexpressed IGF-IRs, by promoting the aggregation, growth, and survival of breast cancer cells, may accelerate the increase of tumor mass and may also prevent cell scattering. © 1997 Academic Press

The insulin-like growth factor I receptor (IGF-IR)² belongs to the tyrosine kinase receptor superfamily [1]. Upon ligand binding, the intrinsic tyrosine kinase of the IGF-IR is activated, which results in the immediate tyrosine phosphorylation of several cellular substrates. Two well-characterized substrates are insulin receptor substrate-1 (IRS-1) and SHC [2–5]. Both act as docking proteins, recruiting different effector molecules and activating multiple signaling systems, for instance, the pathways of Ras or PI-3 kinase. Ultimately, some of the IGF-IR-induced signals stimulate nuclear events, while others are involved in the reorganization of cell morphology [2–9].

Several lines of evidence support an important role of the IGF system (the IGF-IR, its ligands, and IGF-binding proteins) in breast cancer. IGF-I and IGF-II are potent mitogens for cultured breast cancer cells [10] and the levels of the IGF-IR are significantly higher in breast tumors than in normal breast tissue [11]. In primary breast cancer, a correlation has been found between tumor size, the levels of IRS-1, and recurrence of the disease [12]. In estrogen-responsive breast cancer cells, physiological concentrations of estradiol (E2) upregulate the expression of IGF-IRs [13, 14], IGF-II [15], and certain binding proteins [16]. On the other hand, overexpression of IGF-II or IRS-1 renders cells estrogen-independent [14, 17]. Most importantly, blockade of the IGF-IR autocrine or paracrine loop with anti-IGF-IR antibodies, excess of IGF-binding protein, antisense RNA against IGF-IR, or antisense oligonucleotides against IRS-1 inhibits breast cancer growth *in vitro* or *in vivo* [14, 18–20].

The role of the IGF-IR in the metastasis of mammary tumor is not clear. In mouse mammary carcinoma, cells

¹ To whom correspondence and reprints requests should be addressed at Kimmel Cancer Institute BLSB 606A, Thomas Jefferson University, 233S 10th Street, Philadelphia, PA 19107. Fax: (215) 923-0249.

² Abbreviations used: E2, 17- β -estradiol; FACS, fluorescence-assisted cell sorting; IGF-I, insulin-like growth factor I; IGF-IR, IGF-I receptor; IRS-1, insulin receptor substrate 1; MCF-7/IGF-IR, MCF-7 cells overexpressing IGF-IRs; NS, statistically nonsignificant; PCR, polymerase chain reaction; SFM, serum-free medium; PRF-SFM, phenol red-free SFM.

with higher levels of IGF-IRs are more metastatic [21]. On the other hand, based on the studies on IGF-IR content in breast tumors, it has been postulated that higher levels of the receptor are associated with a more favorable clinical outcome and may reflect a more differentiated breast cancer phenotype [11].

It is well established that in breast cancer cells, the acquisition of a metastatic phenotype may be related to deterioration or deactivation of adherens-type cell junctions. These types of junctions are structured around transmembrane cadherin proteins [22–26]. The strength of cadherin-mediated adhesion is regulated by different cytoplasmic catenins which connect cadherins to the actin filament network [24]. E-cadherin is often expressed in breast epithelial cells [22–24] and its presence usually correlates with a nonmetastatic phenotype [23–25]. On the other hand, loss or downregulation of E-cadherin has been observed in several metastatic breast cancer cell lines [23–25]. In several studies, restoration of E-cadherin function, by overexpression of this molecule or by treatment with growth factors or other compounds, resulted in increased adhesion and reduced metastasis [26–29]. Thus, an invasion suppressor role for E-cadherin has been postulated [28].

Here we report that in MCF-7 breast cancer cells, overexpressed IGF-IRs reduce estrogen requirements for growth and enhance responsiveness to low concentrations of IGF-I in the presence of E2. We also demonstrate that high levels of the IGF-IR promote cell–cell adhesion, allow proliferation of cells within aggregates, and protect clustered cells from death.

MATERIALS AND METHODS

IGF-IR expression plasmid. The pcDNA3/IGF-IR expression vector contains a full human IGF-IR cDNA [1] cloned into *Xho*–*Xba* polylinker sites of the pcDNA3 expression plasmid (Invitrogen). The expression of IGF-IR cDNA is driven by the CMV promoter. The plasmid also encodes a neomycin resistance gene.

Development of cell lines and cell culture conditions. MCF-7 cells were routinely grown in DMEM:F12 (1:1) containing 5% CS. In experiments that required estrogen-free conditions, cells were cultured in phenol red-free DMEM containing 0.5 mg/ml BSA, 1 μ M FeSO₄, and 2 mM L-glutamine (PRF-SFM).

The MCF-7/IGF-IR cell lines used in this study were developed by stable transfection with plasmids pcDNA3/IGF-IR or pcDNA3, followed by selection in medium containing 2 mg/ml G418. The neomycin-resistant clones were then screened by PCR. MCF-7/IGF-IR clones were maintained in culture for no longer than 3 months in the above medium with addition of 200 μ g/ml G418.

PCR. The incorporation of the IGF-IR cDNA into MCF-7 cells' genome was assessed by PCR. Briefly, DNA was isolated from 1000 to 10,000 cells. A fragment of the IGF-IR DNA was amplified using the following primers: upstream primer (located in the exon I of the IGF-IR coding sequence) 5'-AAG GAA TGA AGT CTG GCT CC-3'; downstream primer 5'-CTC GAT CAC CGT GCA GTT CT-3' (in exon II). Using these primers we were able to discriminate between the endogenous and the transfected IGF-IR DNAs. The conditions of PCR were 35 cycles of denaturation at 94°C for 1 min, annealing at

55°C for 1 min, extension at 72°C for 1 min; the last extension was for 6 min. The size of the DNA fragment amplified from the transfected IGF-IR cDNA was 170 bp.

FACS. To estimate the level of the IGF-IR in each of the MCF-7/IGF-IR clones, we used fluorescence-activated flow cytometry sorting (FACS) [30]. Briefly, the cells were cultured for 3 days in PRF-SFM (to downregulate endogenous receptors). Then the cells were trypsinized, washed with ice-cold PBS, and incubated for 30 min at 4°C in PBS containing 10 μ g/ml of an anti-IGF-IR antibody (alpha-IR3, Oncogene Science). Next, the cells were washed with ice-cold PBS and incubated in the dark for 30 min at 4°C with 2 μ g/ml of an FITC-conjugated goat anti-mouse IgG (Oncogene Science). Unbound antibody was removed by washing with PBS and the level of fluorescence was determined with EPICS Profile Analyzer. The primary antibody was omitted in control experiments.

Scatchard analysis. The number of the IGF-IR and ligand/receptor dissociation constant was determined by ligand replacement assay [30]. Briefly, the cells were plated at 1×10^5 cells per well in a 12-well plate in DMEM:F12 containing 5% CS. Next day, the cells were shifted to PRF-SFM for 3 days. Then, the cells were washed with DMEM and incubated for 6 h at 4°C in binding buffer [30] containing 0.1 nM ¹²⁵I-IGF-I (NEN/DuPont) and increasing concentrations of unlabeled IGF-I (at a range 0.0–5.0 nM). Next, the cells were washed three times with PBS containing 1 mg/ml BSA and lysed with 0.03% SDS. Cell-bound radioactivity was measured using a gamma counter. Nonspecific binding was determined in the presence of 33.0 nM unlabeled IGF-I. The binding characteristic was analyzed by the LIGAND program. For all tested cell lines, the best fit of binding was obtained with a one-site model.

Binding competition assay. The IGF-I binding assay was performed in the presence of insulin [31]. The cells were plated and synchronized in SFM as described for Scatchard analysis and then incubated with 0.1 nM ¹²⁵I-IGF-I and unlabeled insulin at concentrations from 0.01 to 100 nM. The same amounts of unlabeled IGF-I were used in control experiments. The amount of cell-bound ¹²⁵I-IGF-I was determined as described above.

Western blotting and immunoprecipitation. The levels of IGF-IR, IRS-1, SHC, and E-cadherin, as well as the levels of tyrosine phosphorylation of these proteins, were measured by Western blotting. The cells were cultured as described in the figure legends and then lysed, as described in Refs. [30, 32]. The protein lysate (300–1000 μ g) was immunoprecipitated with an appropriate antibody. The following antibodies were used for immunoprecipitation: for IGF-IR, an anti-IGF-IR monoclonal antibody alpha-IR3 (Oncogene Science); for IRS-1, an anti-IRS-1 polyclonal antibody (UBI); for SHC, an anti-SHC polyclonal antibody (Transduction Laboratories); and for E-cadherin, an anti-E-cadherin monoclonal antibody (Transduction Laboratories). The immunoprecipitates were resolved by PAGE and the proteins were immunodetected with the appropriate antibody. For IRS-1, SHC, and E-cadherin, the antibodies were the same as used for immunoprecipitation. To detect the IGF-IR, we used an anti-IGF-IR polyclonal antibody (Santa Cruz). Tyrosine phosphorylation of the above proteins was detected by immunoblotting with an anti-phosphotyrosine monoclonal antibody PY20 (Transduction Laboratories). The amounts of proteins were estimated by laser densitometry reading. Tyrosine phosphorylation level of E-cadherin-associated proteins was measured 72 h after stimulation (which was the time necessary to complete and stabilize cell–cell aggregation).

[³H]Thymidine incorporation. Cells were plated into 96-well plates at a concentration of 1×10^4 cells per well in DMEM:F12 containing 5% CS and were grown until 80% confluent. Then, the medium was replaced with PRF-SFM containing 10 nM tamoxifen (to synchronize the cells in quiescence). After 3 days, the cells were washed twice with PRF-SFM and incubated in PRF-SFM supplemented with different amounts of IGF-I, E2, or IGF-I + E2 for 18–20 h. Next, the cultures were pulsed with 0.5 μ Ci/well of [³H]thymidine for 4 h. The amount of radioactivity incorporated into

trichloroacetic acid-insoluble material was counted using a beta counter (1209 Rackbeta, Wallac). The stimulation of [³H]thymidine incorporation into DNA was calculated as follows: cpm's obtained in unstimulated cells (PRF-SFM) were taken as basal value equaling 100%; cpm's in cells stimulated with either IGF-I, E2, or IGF-I + E2 were expressed as the percentage increase over basal level.

The sensitivity index ED₅₀ was calculated as described in Ref. [33].

Soft agar assay. The anchorage-independent growth was determined by soft agar assay as described previously [14]. The growth of cells was tested in semisolid DMEM:F12 medium supplemented with either 10 or 2% FBS, as well as in PRF-SFM supplemented with 200 ng/ml IGF-I. Colonies of a size greater than 150 μ m were counted after 2 and 3 weeks.

Aggregation on Matrigel. Matrigel (Biocoat/Fisher) was reconstituted according to the manufacturer's instructions. The matrix (200 μ l/well) was placed in a 24-well plate and allowed to solidify. A cell suspension of 2×10^4 cells in DMEM:F12 plus 5% CS was plated in each well and cultured for up to 21 days. The cultures were photographed at Days 5 and 11. At Day 16, the cells were released from the matrix using Dispase (Biocoat/Fisher), stained with trypan blue, and counted in a hemocytometer.

In several experiments, the cells were cultured on Matrigel in the presence of 50 ng/ml IGF-I to assess the ligand-dependent increase of aggregation. The requirement for E-cadherin was tested with the anti-E-cadherin antibody HECD-1 (Zymed) which was added at the time of plating at a concentration of 10 μ g/ml.

Invasion assay. The invasiveness of MCF-7/IGF-IR cells was studied using 24-well invasion chambers (Biocoat/Fisher). Cells (2×10^4) suspended in DMEM:F12 with 5% CS were placed in the upper chamber and cultured for 24 or 48 h. Lower chambers contained the same growth medium. The number of cells that invaded the extracellular matrix and migrated to the underside of the chamber was determined by direct counting (after staining with 0.5% crystal violet). In several experiments, the medium in the lower chamber was supplemented with IGF-I (50–200 ng/ml) or E2 (10 nM) used as chemoattractants.

Immunofluorescence microscopy. The double staining for the IGF-IR and E-cadherin was performed on monolayer cultures of MCF-7 and MCF-7/IGF-IR cells. The localization of the IGF-IR was detected using indirect immunofluorescence, as recommended by Transduction Laboratories (protocol 9). Briefly, 70% confluent cells grown on glass coverslips were fixed for 10 min at room temperature (RT) in 3.7% formaldehyde, washed with PBS, treated with 0.2% Triton X-100 for 5 min, and then blocked in 0.2% BSA for 5 min. The fixed cells were incubated for 1 h at RT with 10 μ g/ml of a rabbit polyclonal anti-human IGF-IR antibody (Santa Cruz), washed with PBS, and incubated with an anti-rabbit-lissamine/rhodamine-conjugated goat IgG (26 μ g/ml) for 30 min. The localization of E-cadherin determined on the same slides using a monoclonal antibody HECD-1 (10 μ g/ml) and a goat anti-mouse IgG-FITC-conjugated (2 μ g/ml). The primary antibodies were omitted in control experiments.

Statistical analysis. The statistical evaluation of results was done using ANOVA single-factor analysis of variance. The significance level was taken as $P \leq 0.05$.

RESULTS

Development of MCF-7/IGF-IR clones. The MCF-7/IGF-IR clones were developed by stable transfection of MCF-7 cells with the pcDNA3/IGF-IR expression vector. The transfected cells were selected in 2 mg/ml G418. Forty-four G418-resistant clones were analyzed by PCR to detect the cells with the integrated IGF-IR plasmid and by FACS to identify the clones that

overexpressed the IGF-IR. Ultimately, five MCF-7/IGF-IR clones were obtained, designated C-12, C-34, C-21, C-17, and C-15. In parallel, by stable transfection of MCF-7 cells with the pcDNA3 vector, we generated control clones MCF-7/pc 2 and MCF-7/pc 4.

The number of IGF-I receptors in MCF-7/IGF-IR clones was determined by Scatchard analysis (Fig. 1B). The cells were incubated for 4 days in phenol red-free serum-free medium (PRF-SFM) to ensure downregulation of endogenous IGF-IRs in the absence of E2. The IGF-IR content in MCF-7/IGF-IR clones ranged from 0.5×10^6 to 3.0×10^6 receptors/cell, which represented an 8- to 50-fold increase over the IGF-IR level in MCF-7 cells (0.6×10^5 receptors/cell) [14] (Figs. 1A and B). The number of receptors in the control MCF-7/pc 2 and pc 4 clones was slightly lower than that in the parental cells (0.3×10^5 and 0.4×10^5 sites/cell, respectively) but the differences did not reach statistical significance. The dissociation constant (K_d) in all clones was in the range of K_d values reported for IGF-I/IGF-IR binding [34–36] (Fig. 1A). In addition, in order to rule out the possibility that the increased number of binding sites was due to selective formation of IGF-I/insulin hybrid receptors [31], binding competition assays with insulin were performed. In the all MCF-7/IGF-IR clones, IGF-I binding was not displaced even with very high (100 nM) concentrations of insulin (data not shown).

Figure 1C demonstrates the IGF-IR levels in MCF-7/IGF-IR clones by FACS. Compared with MCF-7 cells, the increase in relative IGF-IR fluorescence in MCF-7/IGF-IR clones was from 2.5- to 25.1-fold. MCF-7/pc 2 and pc 4 clones exhibited fluorescence similar to that in MCF-7 cells (0.9 and 0.95 of the level in the parental cells).

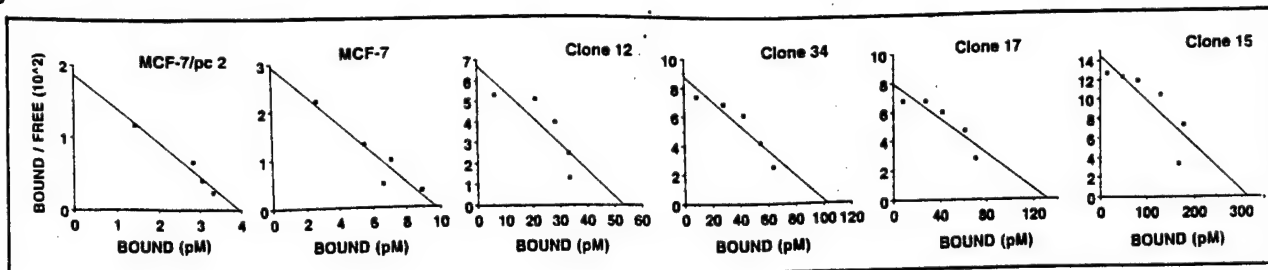
Additionally, the level of the IGF-IR protein in the developed clones was assessed by immunoprecipitation and subsequent immunoblotting with an anti-IGF-IR antibody (Fig. 2A). The increase of the IGF-IR beta-subunit in the clones C-12, C-34, C-21, C-17, and C-15 compared with that in MCF-7 cells was 2-, 5-, 7-, 10-, and 21-fold, respectively (estimated by laser densitometry). The levels of IGF-IR protein in clones MCF-7/pc 2 and pc 4 were similar to those in MCF-7 cells and were barely detectable by Western blotting (not shown).

In MCF-7/IGF-IR clones, both basal and IGF-I-induced tyrosine phosphorylation of the IGF-IR and IRS-1 were markedly increased compared with the levels in the parental cells. The representative experiment, involving clones with the highest overexpression of the receptor, is shown in Fig. 2B. In MCF-7/IGF-IR clones 15 and 17, the levels of tyrosine phosphorylation of the IGF-IR were consistently at least 4-fold higher in cells treated for 5 min with IGF-I, and at least 8-fold higher under SFM, than the corresponding levels in MCF-7

A

Cells	MCF-7/pc 2	MCF-7	Clone 12	Clone 34	Clone 21	Clone 17	Clone 15
N_R	0.03×10^6	0.06×10^6	0.5×10^6	0.9×10^6	0.8×10^6	1.1×10^6	3.0×10^6
K_d	0.21	0.28	0.79	1.16	0.47	1.65	2.1
K_{FACS}	0.9	1.0	2.5	2.8	6.9	12.6	25.1

B



C

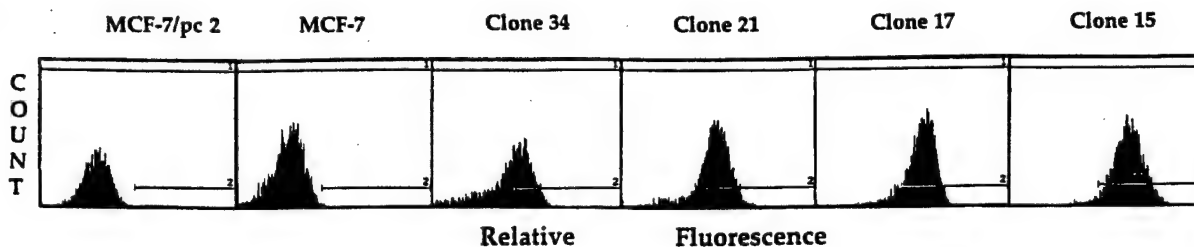


FIG. 1. Characteristics of MCF-7/IGF-IR clones. (A) Summary of parameters: IGF-IR number (N_R), dissociation constant K_d (nM), and relative fluorescence index (K_{FACS}). Binding parameters were determined, and FACS analysis was performed, as described under Materials and Methods. K_{FACS} represents the fold increase of the relative IGF-IR fluorescence in MCF-7/IGF-IR clones over that in MCF-7 cells. (B) Scatchard analysis. Abscissa, bound IGF (pM); ordinate, bound/free IGF $\times 10^{-2}$. The binding experiments for each clone were repeated at least three times. The representative Scatchard plots are shown. (C) FACS analysis. Abscissa, relative IGF-IR fluorescence; ordinate, cell number. In each experiment, 5×10^3 of cells were analyzed. Each analysis was performed at least two times. The representative results are shown. In control experiments, where cells were stained with secondary antibody only, the level of fluorescence was undetectable.

cells (estimated by laser densitometry). The tyrosine phosphorylation of IRS-1 was also more pronounced in MCF-7/IGF-IR clones than in the parental cells: specifically, at least 2-fold greater under IGF treatment, and from 1.6- (clone 12) to 6-fold (clone 15) greater in SFM (Fig. 2C). In the latter case, presumably due to a low concentration of ligand, there was an apparent correlation between tyrosine phosphorylation of IRS-1 and the number of IGF-IRs. In the presence of IGF-I, the saturation of IRS-1 stimulation was obtained in clone 12 expressing 5×10^6 receptors/cell. The levels of IRS-1 protein in the studied cells were similar under all experimental conditions (not shown).

E2 responsiveness in MCF-7/IGF-IR cells. MCF-7 cells and all developed MCF-7/IGF-IR clones responded similarly to E2 with stimulation of [3 H]thymidine incorporation into DNA (data not shown). In all cell lines, 0.05 nM E2 yielded a maximal response (a 2.9- to 6.8-fold increase over the basal level), while concentrations

up to 1.0 nM had no additional effect. The differences in E2 responsiveness observed among the tested clones were not statistically significant. E2 at a concentration higher than 20.0 nM exerted an inhibitory effect. Consequently, a concentration of 0.1 nM E2 was used in all further experiments.

Sensitivity and responsiveness of MCF-7/IGF-IR cells to IGF-I alone or in combination with E2. The overexpression of IGF-IR did not modify sensitivity to IGF-I (evaluated by [3 H]thymidine incorporation into DNA) (Fig. 3). Specifically, the ED_{50} for MCF-7 was 0.56 ng/ml and for MCF-7/IGF-IR cells it ranged from 0.42 to 0.67 ng/ml, $P = NS$. The responsiveness to IGF-I, however, was increased in most MCF-7/IGF-IR clones. For instance, with 4 ng/ml IGF-I, there was a 325% increase of [3 H]thymidine incorporation in MCF-7 cells, whereas increases of 336, 492, 580, 728, and 648% were observed in clones C21, C12, C34, C17, and C15, respectively.

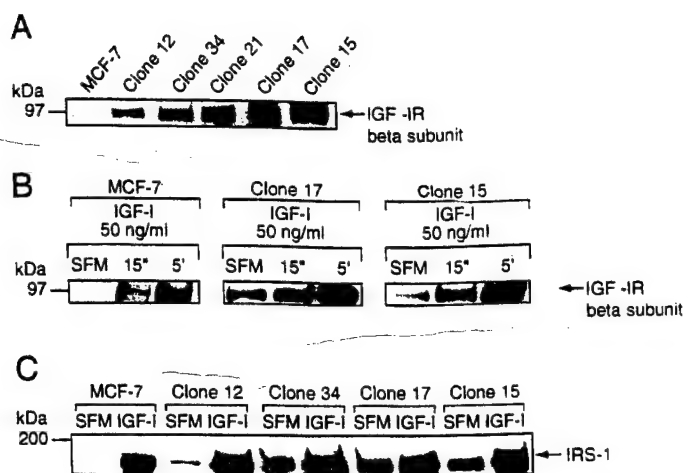


FIG. 2. Activation of IGF-IR signaling in MCF-7/IGF-IR cells. (A) IGF-IR protein levels. The IGF-IR protein level in MCF-7 cells and clones 12, 34, 21, 17, and 15 was determined by immunoprecipitation with an anti-IGF-IR antibody and subsequent Western immunoblotting, as described under Materials and Methods. 300 μ g and 1 mg of proteins were used to immunoprecipitate the IGF-IR from MCF-7/IGF-IR and MCF-7 cells, respectively. The analysis was performed at least two times for each clone. (B) Tyrosine phosphorylation of the IGF-IR. Cells were incubated in PRF-SFM for 3 days and then stimulated with 50 ng/ml IGF-I for 15 s or 5 min. Tyrosine phosphorylation of the IGF-IR was measured by immunoprecipitation with an anti-IGF-IR antibody followed by Western immunoblotting with an anti-phosphotyrosine antibody. The experiments were repeated at least four times; representative results for MCF-7 cells, clone 17, and clone 15 are shown. (C) Tyrosine phosphorylation of IRS-1. Cells were grown in PRF-SFM for 3 days with or without 50 ng/ml of IGF-I. 300 μ g of lysate was immunoprecipitated with an anti-IRS-1 antibody and immunoblotted with an anti-phosphotyrosine antibody. The experiments were repeated at least two times; representative results are presented.

In MCF-7 cells, 0.1 nM E2 combined with IGF-I (0.01–100 ng/ml) produced a synergistic effect on [3 H]-thymidine incorporation. In contrast, in all MCF-7/IGF-IR clones, E2 increased the mitogenic response only in the presence of low concentrations of IGF-I (less than 1 ng/ml). With larger amounts of IGF-I, the synergistic effect of E2 was abolished, and IGF-I alone was sufficient to maximally stimulate DNA synthesis (Fig. 3). The effect of IGF-I alone or in combination with E2 on DNA synthesis in MCF-7/pc clones was similar to that found for MCF-7 cells (not shown).

Overexpression of the IGF-IR does not improve the ability of MCF-7 cells to grow in soft agar or in monolayer culture. The ability of MCF-7/IGF-IR clones to grow under anchorage-independent conditions was similar to that exhibited by MCF-7 and MCF-7/pc cells. Specifically, all tested cell lines formed approximately 100 colonies in soft agar containing 10% FBS, 120 colonies in agar with 10% FBS plus 200 ng/ml IGF-I, and 45 colonies in agar with 2% FBS. In addition, similarly to the parental cell line, none of the MCF-7/IGF-IR

cells produced colonies greater than 100 μ m in semi-solid PRF-SFM supplemented with 200 ng/ml IGF-I.

In monolayer culture, the increase in cell number was similar in all studied cell lines, regardless of the level of IGF-IR overexpression. Specifically, 72 h after stimulation with IGF-I (0.1–10 ng/ml), in all cases, the number of cells increased $\sim 1.7 \pm 0.3$ -fold (data not shown).

Overexpression of the IGF-IR does not induce invasiveness of MCF-7 cells in vitro. MCF-7 cells have been reported as noninvasive or poorly invasive [27]. We found that the overexpression of IGF-IR in MCF-7 cells did not alter their noninvasive phenotype *in vitro*. Using invasion chambers (Biocoat/Fisher), we noted that only approximately 0.2% cells were able to traverse the extracellular matrix. Additionally, invasiveness of the cells was not stimulated when IGF-I or the combination of IGF-I + E2 was used as chemoattractant.

Overexpression of the IGF-IR stimulates cell-cell adhesion in MCF-7 cells. MCF-7 cells cultured on Matrigel (extracellular matrix) formed globular aggregates characteristic of a noninvasive phenotype [27]. As shown in Fig. 4, cell aggregation was significantly stimulated in clones overexpressing the IGF-IR. The extent of aggregation appeared to parallel the increase of the IGF-IR number in the cells (Figs. 4a–4e). For instance, at Day 5 of culture, MCF-7 cells did not produce any aggregates of a size greater than 150 μ m, whereas the clones C-12 and C-34 (Figs. 4b and 4c) formed an average of 8 and 10 such aggregates, respectively. The clones 17 and 15 (Figs. 4d and 4e) produced a few clusters of a size greater than 300 μ m and several smaller aggregates of the size 150–300 μ m. The average results from five experiments were as follows: for clone C-17, there were 4 aggregates greater than 300 μ m and 5 of the size 150–300 μ m, and for clone 15, there were aggregates greater than 300 μ m and 7 of the size 150–300 μ m.

When culture on Matrigel was extended up to 21 days, MCF-7 cells and the clones expressing less than 1.1×10^6 IGF-IRs progressively disaggregated and died (Fig. 4f–4h). At Day 16 of the experiment, of 2×10^4 initially plated cells, we found an average of 1.2×10^2 , 1×10^2 , and 8×10^3 viable cells for MCF-7, clone 34, and clone 12, respectively. In contrast, the clones expressing the highest levels of the IGF-IR not only remained well aggregated, but also proliferated in compact clusters (Figs. 4i–4j). Indeed, at Day 16, the number of cells was even increased up to 1.1×10^5 cells for clone 17 and to 4.6×10^4 cells for clone 15.

The aggregation and survival of MCF-7/pc 2 and pc 4 cells cultured on Matrigel was similar to that noted for the parental cells. The morphology and size of the clusters produced by MCF-7/pc 2 cells is shown in Fig. 5A.

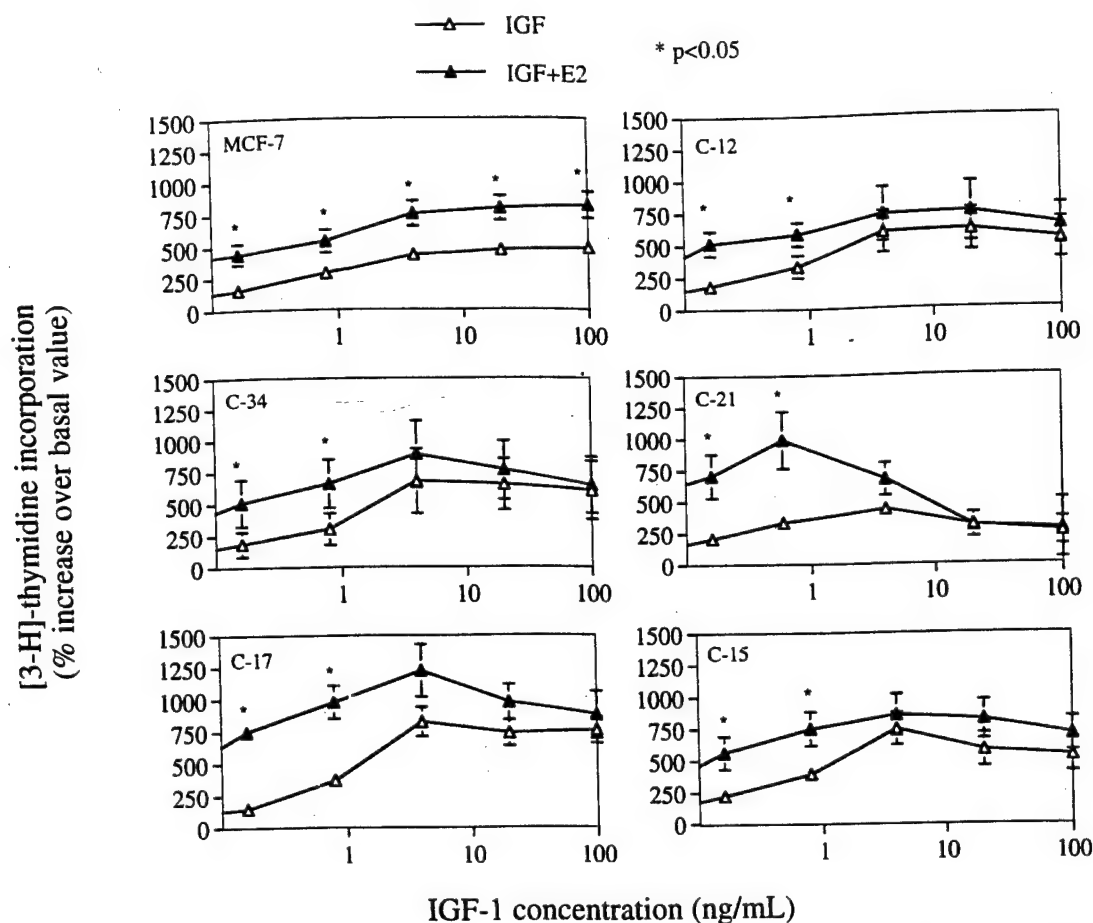


FIG. 3. Stimulation of [3 H]thymidine incorporation by IGF-I alone or in combination with E2 in MCF-7 and MCF-7/IGF-IR cells. The cells were synchronized and stimulated with different amounts of IGF-I with or without 0.1 nM E2, as described under Materials and Methods. Abscissa, tested concentrations of IGF-I. Ordinate, percentage increase of [3 H]thymidine incorporation (in cpm) over basal level (cpm values in untreated cells). The values are means from at least four experiments. Bars, SE. Asterisks indicate statistically significant differences between IGF-I and IGF-I plus E2 values by ANOVA ($P < 0.05$).

IGF-I stimulates aggregation of MCF-7 and MCF-7/IGF-IR cells: Anti-E-cadherin antibody blocks the formation of aggregates. In the presence of 20 ng/ml IGF-I, MCF-7 cells as well as MCF-7/IGF-IR clones displayed increased aggregation on Matrigel. As shown in Fig. 5, the size of average aggregates typically increased from approximately 100 to 150 μ m in MCF-7 cells (Fig. 5B, parts a and c), and from 180 to 250 μ m in clone 15 (Fig. 5B, parts b and d). In contrast, in all studied cell lines, the addition of an anti-E-cadherin antibody at the time of cell plating effectively blocked cell-cell adhesion. The effect of anti-E-cadherin antibody on aggregation in MCF-7 cells and in MCF-7/IGF-IR clone 15 is presented in Fig. 5B, parts e and f.

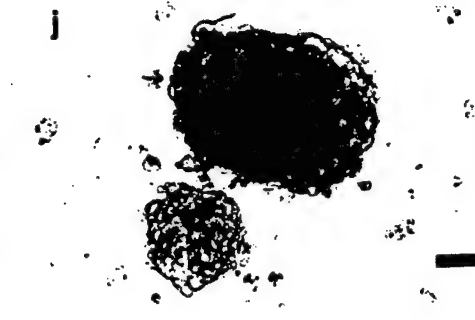
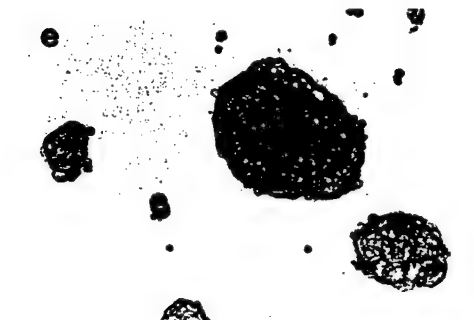
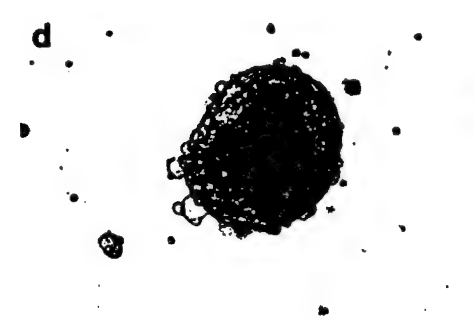
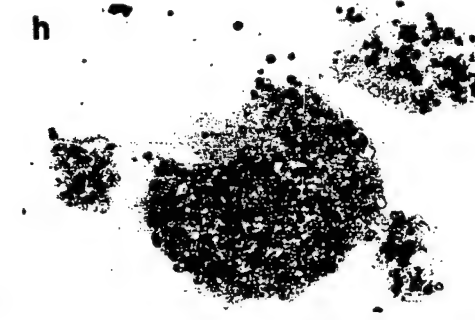
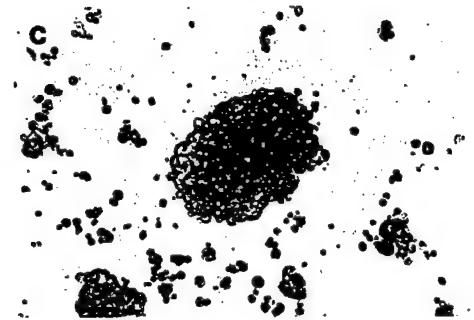
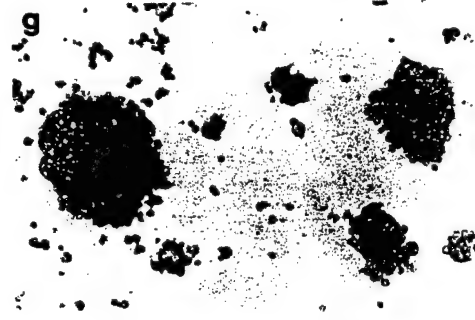
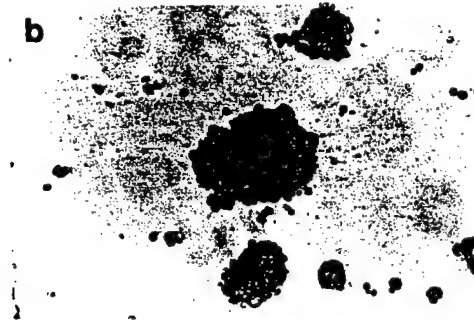
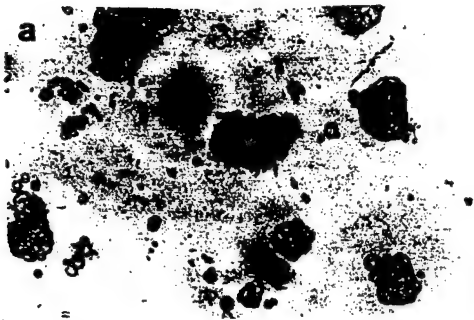
The IGF-IR co-localizes with E-cadherin in MCF-7/IGF-IR cells. The IGF-IR and E-cadherin were detected by double-staining with specific antibodies. In MCF-7 cells, immunofluorescence analysis with an anti-IGF-IR antibody produced barely visible staining on the cell surface (Fig. 6a), while immunodetection with anti-E-cadherin antibody revealed the typical E-cadherin honeycomb pattern [25] (Fig. 6b).

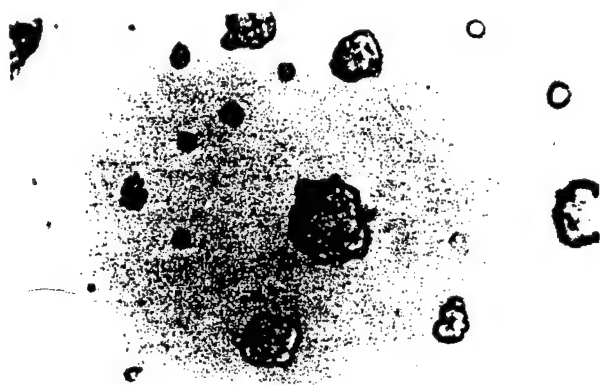
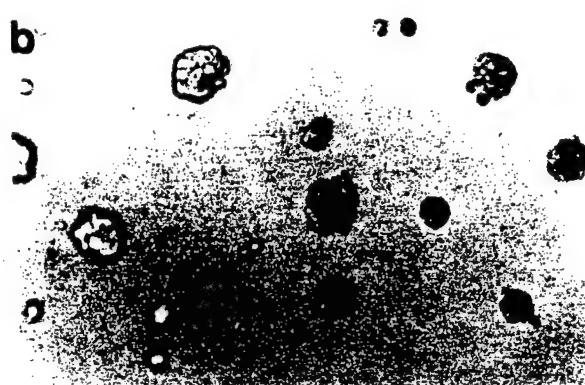
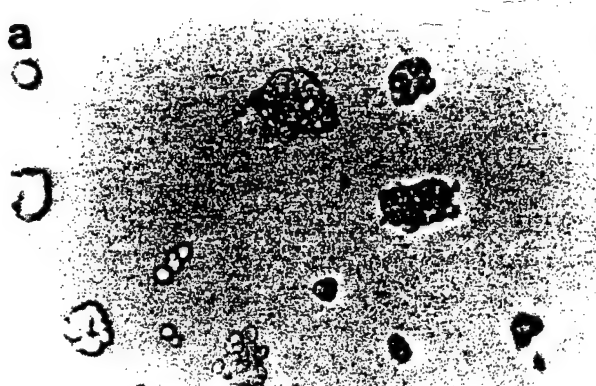
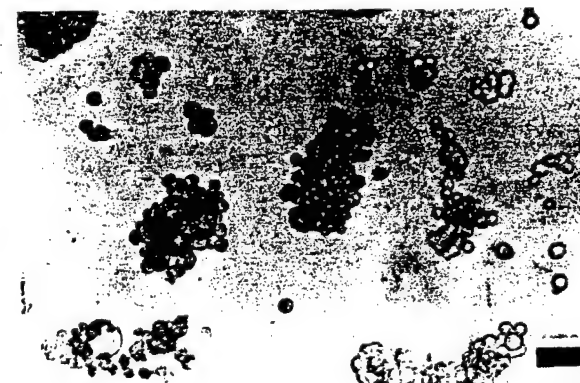
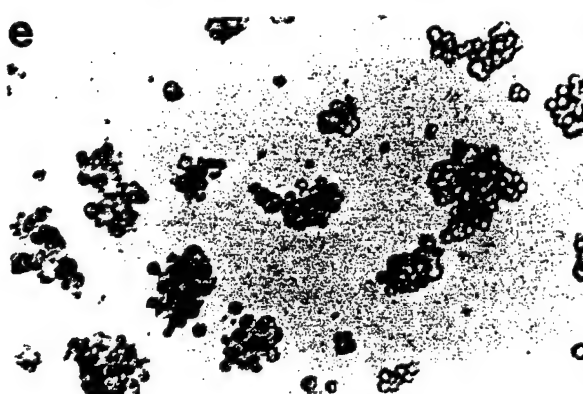
In MCF-7/IGF-IR clones, the IGF-IR was easily detectable by immunofluorescence. The staining appeared to be concentrated at areas of cell-cell contacts (Figs. 6c and 6e), which was particularly evident in clones with very high receptor content (Fig. 6e). Remarkably, in MCF-7/IGF-IR clones, the IGF-IR co-lo-

FIG. 4. Aggregation of MCF-7/IGF-IR cells. 20,000 cells were plated on Matrigel. The morphology of the clones was recorded by phase-contrast microscopy after 5 and 11 days of culture. MCF-7 cells (a, f); clone 12 (b, g); clone 34 (c, h), clone 17 (d, i); clone 15 (e, j). Bar, 100 μ m. The experiments were repeated at least four times for all analyzed cells. The representative results are shown.

Day 5

Day 11



A**b****B****a****c****e**

calized with E-cadherin (Figs. 6d and 6f). Interestingly, in contrast to the uniform membrane distribution of E-cadherin in MCF-7 cells, the localization of this protein appeared to be altered in cells with very high IGF-IR content. Specifically, more E-cadherin tended to accumulate in the areas of cell membranes containing the highest amounts of the IGF-IR (Figs. 6e and 6f).

IGF-IR, IRS-1, and SHC associate with E-cadherin. We further investigated whether the IGF-IR and associated substrates physically interact with E-cadherin complexes. Figure 7 shows representative data from several independent experiments. Figure 7A demonstrates patterns of tyrosine phosphorylation of proteins coprecipitating with E-cadherin in MCF-7 cells and in clones 12, 17, and 15 cultured under various conditions. In all analyzed cells, the patterns of tyrosine phosphorylated proteins associated with E-cadherin were similar (Fig. 7A) and contained at least seven distinct bands. The most prominent were the bands of the approximate sizes 95, 185, and 200 kDa (the last not seen in MCF-7 cells). In the following experiments, we examined, by reprobing the blots with different antibodies, whether E-cadherin-associated proteins contain the elements of the IGF-I signaling pathway. Due to multiple stripping and reprobing, we were not always able to demonstrate the levels of all studied proteins in each individual blot. However, in several independent experiments, we confirmed the presence of each of the IGF-IR signaling molecules, the IGF-IR, IRS-1, and SHC, in E-cadherin complexes of all studied cells (not shown).

Figure 7B demonstrates the amounts of E-cadherin, IRS-1, IGF-IR, or SHC in the precipitates. E-cadherin, as expected, was detectable in all precipitates. In MCF-7 cells, a 185-kDa band noticeable in cells treated with IGF-I (Fig. 7A) contained IRS-1. IRS-1 was also present in E-cadherin precipitates of other cells (shown here for clone 15). In contrast to MCF-7 cells, however, tyrosine phosphorylation of IRS-1 in MCF-7/IGF-IR clones 12, 17, and 15 was also noticed under SFM or 5% CS conditions.

The E-cadherin complexes contained the IGF-IR (shown here for MCF-7 cells, clone 12, and clone 17). Relative to E-cadherin levels, the amount of IGF-IRs in the complexes appeared to be greater in cells overexpressing the receptor (see clones 12 and 17, compared with MCF-7 cells). The extent of tyrosine phosphorylation of the IGF-IR was impossible to determine since the phosphorylated band of the size 95 kDa contained

not only the IGF-IR but also large amounts of β -catenin which was phosphorylated on tyrosine residues (not shown).

The tyrosine phosphorylation of E-cadherin was low and was further reduced (approximately 50%) in MCF-7, clone 12, and clone 15, as a result of 72 h of IGF-I treatment (Fig. 7). In several experiments, we did not notice any consistent modification of E-cadherin protein expression under IGF-I. The exception was clone 17, in which IGF-I caused a reduction of E-cadherin levels.

SHC proteins complexed with E-cadherin were not phosphorylated on tyrosines under any of the experimental conditions.

DISCUSSION

Although numerous studies [10–20] have suggested an important role for the IGF paracrine or autocrine loop in the regulation of breast cancer growth, the impact of the IGF-IR on the progression of the disease is still largely unknown. Here, we examined whether a substantial increase in the IGF-IR levels would induce processes associated with breast cancer progression, such as increased sensitivity or responsiveness to IGF-I, development of estrogen independence, enhancement of anchorage-independent growth, or induction of invasiveness. In IGF-I- and E2-dependent, noninvasive MCF-7 cells, the overexpression of the IGF-IR produced: (i) a moderate mitogenic effect, reflected by sensitization of cells to low concentrations of IGF-I in the presence of E2 and reduction of E2 requirements with large amounts of IGF-I, and (ii) a marked morphogenic effect, reflected by stimulation of cell-cell adhesion.

Our studies were greatly facilitated by the successful development of MCF-7-derived clones expressing different levels of IGF-IRs. The first part of this work provides characteristics of our experimental model. The expression of IGF-IRs was determined by three independent methods: Scatchard binding assay (Fig. 1B), FACS analysis (Fig. 1C), and Western immunoblotting (Fig. 2). The number of IGF-I binding sites in the developed clones assessed by Scatchard assay was from 8- to 50-fold higher than that in the parental cells (Figs. 1A and 1C). This higher IGF-I binding was not associated with any noticeable overexpression of low-affinity binding sites for IGF-I (likely to represent surface IGF binding proteins [37] (Fig. 1B). Hybrid IGF-I/insulin receptors, with affinity toward both li-

FIG. 5. (A) Aggregation of a control clone. The morphology of control cells MCF-7 (a) and MCF-7/pc2 (b) at Day 5 of culture on Matrigel. Three independent experiments were performed. (B) Effects of IGF-I and anti-E-cadherin antibody on aggregation of MCF-7 and MCF-7/IGF-IR cells. The sizes and morphology of average aggregates produced by MCF-7 cells (a–e) and MCF-7/IGF-IR clone 15 (b–f) cultured in control medium were analyzed on Day 5 of the experiment. In parallel, the cells were grown in the presence of 50 ng/ml IGF-I (MCF-7, c; clone 15, d) or 10 μ g/ml of anti-E-cadherin antibody (HECD 1) (MCF-7, e; clone 15, f).

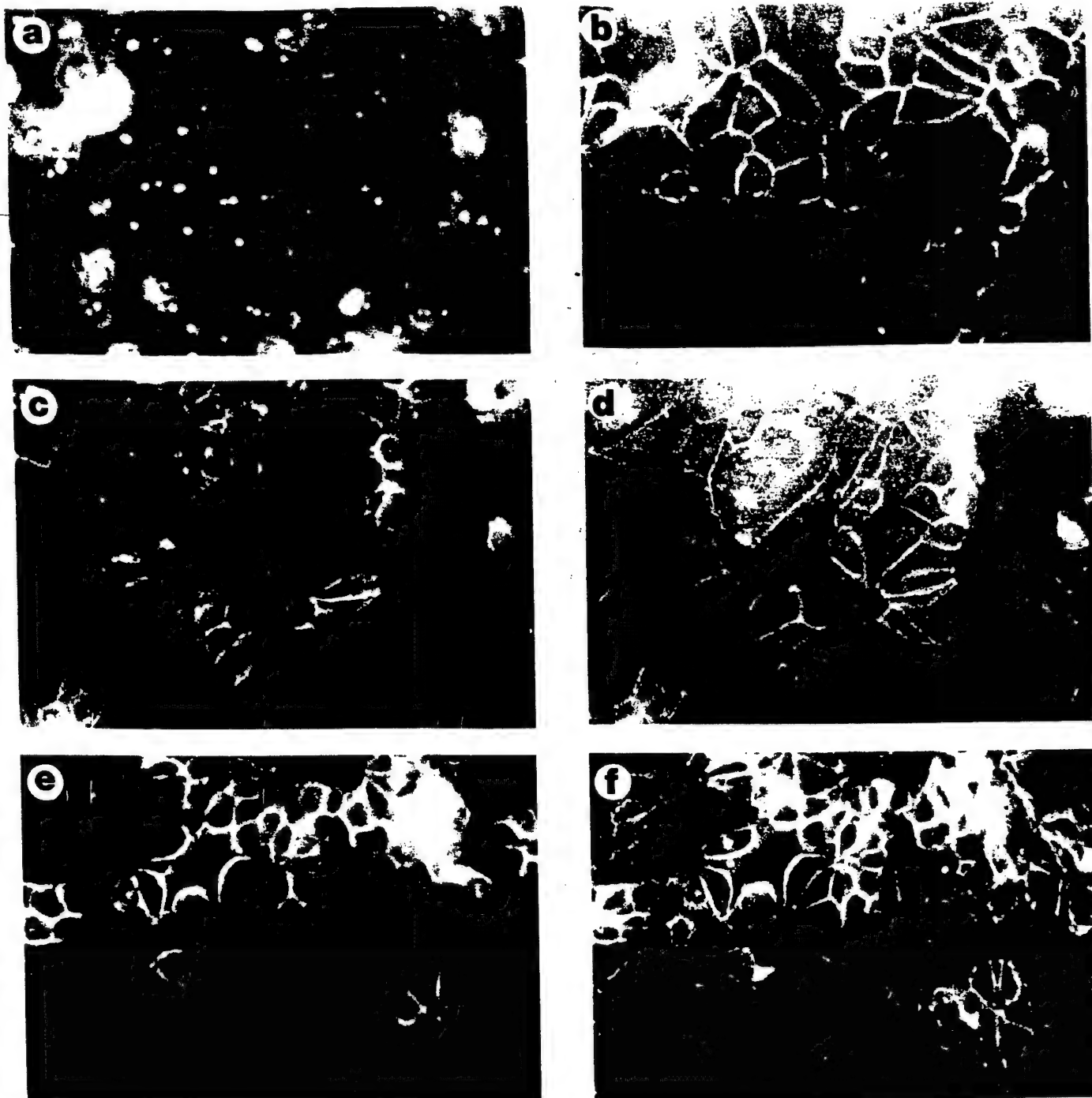


FIG. 6. Co-localization of the IGF-IR and E-cadherin in MCF-7/IGF-IR cells. The IGF-IR was detected with an anti-IGF-IR polyclonal antibody and anti-rabbit rhodamine-conjugated IgG. E-cadherin was localized with an anti-E-cadherin monoclonal antibody (HECD-1) and anti-mouse FITC-conjugated IgG, as described under Materials and Methods. The localization of the IGF-IR in MCF-7 cells (a), clone 12 (c), clone 15 (e) and the staining for E-cadherin in MCF-7 (b), clone 12 (d) and clone 15 (f) were examined and photographed under a Zeiss axiophot microscope with an original magnification of $\times 400$. The arrowheads indicate specific staining. The fluorescence staining observed in the cell nucleoli in a, c, and e was nonspecific.

gands, have been described in many models [31]. We established, by competition binding, that in the MCF-7/IGF-IR clones, IGF-I, but not insulin, was the principal ligand for the overexpressed receptors.

The overexpression of the IGF-IR in MCF-7/IGF-IR cells was further confirmed by two semiquantitative methods, FACS analysis and Western immunoblotting. By FACS, the amount of the IGF-IR protein in the

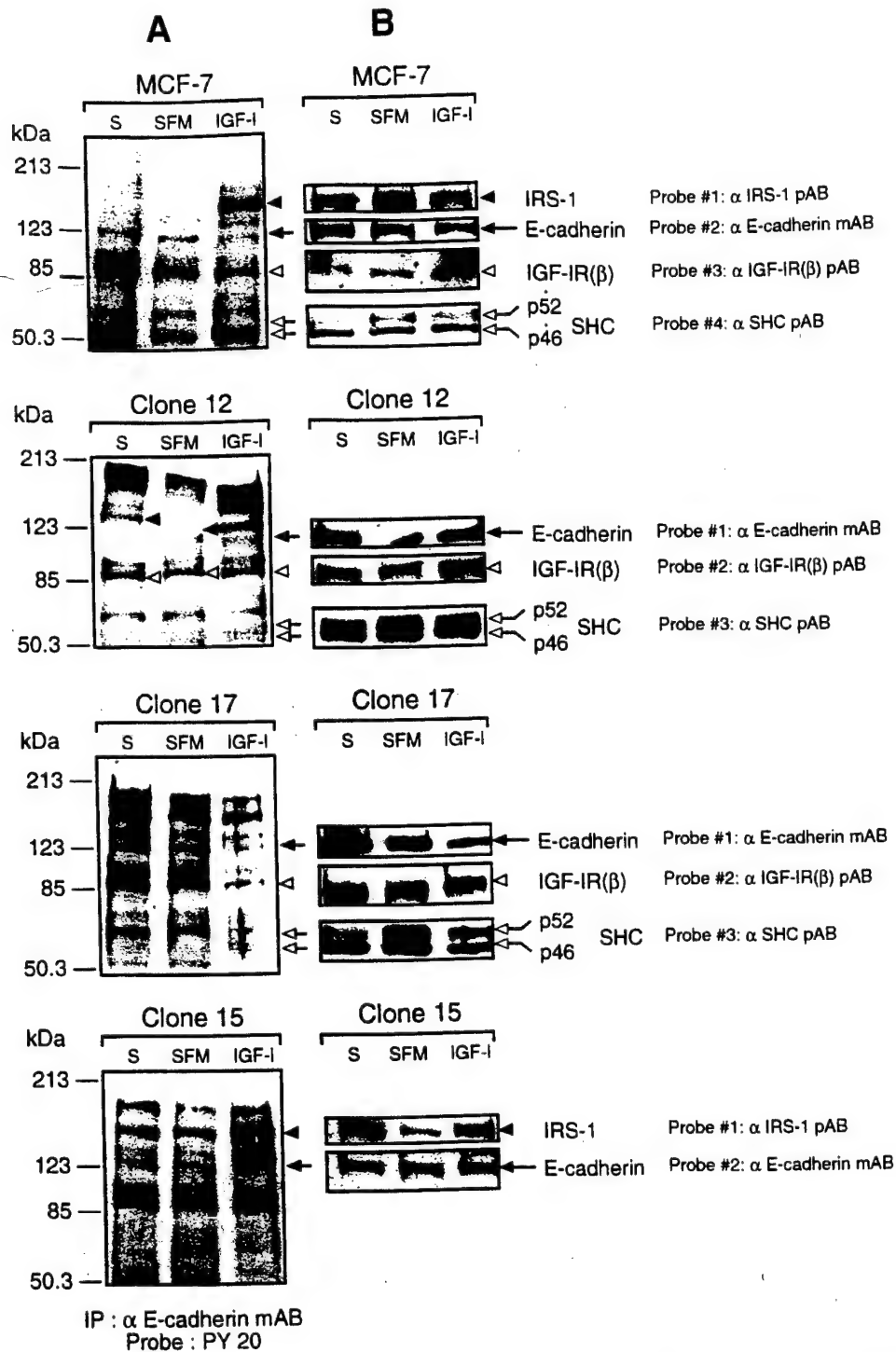


FIG. 7. Association of IGF-I signaling molecules with E-cadherin. Cells were incubated for 3 days in DMEM:F12 with 5% CS (S), PRF-SFM (SFM) or PRF-SFM with 50 ng/ml IGF-I (IGF-I) and then lysed. (A) Tyrosine phosphorylation of E-cadherin-associated proteins. 500 μ g of protein lysate was immunoprecipitated with 4 μ g of an anti-E-cadherin monoclonal antibody. (B) Protein levels of E-cadherin and associated proteins. The immunoblots shown in (A) were stripped and reprobed with an anti-E-cadherin antibody. Next, the membranes were stripped again and reprobed with either an anti-IRS-1 or an anti-IGF-IR antibody. Subsequently, the blots probed with an anti-IGF-IR antibody were stripped and hybridized with an anti-SHC antibody. Due to multiple stripping and the resulting decrease in membrane-bound proteins, we were not able to demonstrate the levels of all studied proteins in a single blot. Note: the E-cadherin and IGF-IR bands in the clone 12 blot were shifted because of a gel crack.

developed clones was elevated from 2.5- to 25.1-fold compared with MCF-7 cells (Fig. 1C); Western blotting revealed a 2- to 21-fold increase (Fig. 2A). Furthermore, we provided evidence that in MCF-7/IGF-IR cells, the extent of IGF-I-induced tyrosine phosphorylation of both IGF-IR and IRS-1 was higher than in MCF-7 cells. Interestingly, a saturation of IGF-stimulated tyrosine phosphorylation was observed. In the case of the receptor, the maximum was seen in cells expressing approximately 1×10^6 sites/cell, whereas expression of 5×10^5 sites/cell produced maximal tyrosine phosphorylation of IRS-1. While the latter may reflect the limited abundance of IRS-1 in cells, the limiting step for the former remains unknown.

All developed clones retained similar sensitivity to E2, which strongly suggested that transfection of MCF-7 cells with the IGF-IR did not affect E2 receptor expression. Similar observations have been reported by other investigators who studied MCF-7 cells overexpressing the EGFR, IGF-IR, or c-erbB-2 [36, 38, 39].

In the next step, we tested monolayer growth of MCF-7/IGF-IR clones with special emphasis on their responsiveness to mitogenic effects of IGF-I and E2. We also examined cell growth under anchorage-independent conditions. Unexpectedly, in all MCF-7/IGF-IR clones, even those with the highest overexpression, the sensitivity to IGF-I was not significantly changed, and the responsiveness to this ligand was only moderately increased, compared with the corresponding parameters in MCF-7 cells. The cells with higher levels of IGF-IRs, however, exhibited increased responsiveness to low concentrations of IGF-I in the presence of E2. With higher concentrations of IGF-I, the synergistic effect of IGF-I and E2 was abolished, despite the fact that the cells retained normal E2 sensitivity. Consequently, in most MCF-7/IGF-IR clones, IGF-I alone, at a concentration of 4 ng/ml, produced the maximal mitogenic effect independent of E2. Our results are in agreement with the recent work of Daws *et al.* [36], who studied MCF-7 cells expressing approximately 2×10^5 IGF-IRs. In these cells, although the combined mitogenic effect of IGF-I and E2 was not increased, an enhanced response to low concentrations of IGF-I in the presence of E2 was noted. Interestingly, in MCF-7/IGF-IR cells, despite moderately increased responsiveness of DNA synthesis to IGF-I, the growth rate (increase of cell number) was not enhanced compared with MCF-7 cells.

These above observations suggest that in breast epithelial cells, the mitogenic effect mediated through the IGF-IR may be a saturated process. The exact nature of this phenomenon is not known. We speculate that in MCF-7/IGF-IR cells, the limited increase of response to IGF-I may be related to the translocation of a significant fraction of IGF-IRs to cell-cell boundaries

where they are not fully accessible for IGF-I stimulation (Fig. 6) (see below).

Under anchorage-independent conditions, partial loss of E2 requirements has been described in breast cancer cell lines overexpressing IGF-II [17] or IRS-1 [14]. In contrast, breast cancer cells overexpressing IGF-IRs generated by Daws *et al.* [36] as well as by our laboratory retained E2 requirement for growth in soft agar. It is possible that in both cases, the extent of receptor overexpression, or the abundance of available receptors, was not sufficient to override E2 dependence. It cannot be excluded, however, that in breast cancer cells, anchorage-independent growth requires activation of specific E2 signaling, which can be overridden by amplified IGF-II or IRS-1 signaling, but not IGF-IR signaling.

In the following part of this work, we assessed invasive properties of MCF-7/IGF-IR cells *in vitro* as well as the effects of IGF-IR overexpression on cell-cell adhesion. MCF-7 cells are poorly invasive [25] but their invasive properties *in vitro* can be enhanced, for instance, by the overexpression of H-ras [37-40]. We demonstrated that overexpression of the IGF-IR did not stimulate invasiveness of MCF-7 cells. In contrast, we observed that high levels of IGF-IRs actually promoted cell-cell adhesion and formation of large organoid-like structures on Matrigel (Fig. 4). Importantly, in this assay, the extent of aggregation (number and sizes of aggregates) paralleled the level of IGF-IRs. Moreover, the cells expressing more than 1×10^6 sites/cell not only survived in the aggregates for the longest period but also continued to multiply within the formed clusters. This suggested that the IGF-IR, by stimulating cell-cell adhesion, promoted proliferation of aggregated cells and protected cells from death.

The role of the IGF-IR in cell-cell adhesion was further substantiated by the evidence that IGF-I stimulated the aggregation of MCF-7 and MCF-7/IGF-IR cells (Fig. 5B). The aggregation of these cells was blocked in the presence of anti-E-cadherin antibody, which demonstrated that IGF-IR-enhanced adhesion requires functional E-cadherin (Fig. 5B). Our findings are consistent with the data of Bracke *et al.* [26], who demonstrated that in the invasive breast cancer cell line MCF-7/6, IGF-I stimulated cell aggregation in the absence but not in the presence of an anti-E-cadherin antibody.

The direct visualization by immunofluorescence microscopy revealed that in MCF-7/IGF-IR cells, the IGF-IR co-localizes with E-cadherin at the points of cell-cell contacts (Fig. 6). To our knowledge, this is the first demonstration of co-localization of the IGF-IR with a cell-cell adhesion molecule. The interaction of the IGF-IR with the E-cadherin complex was also confirmed by Western immunoblotting. Specifically, we found that in MCF-7 cells and MCF-7/IGF-IR clones, E-cadherin

associated with IRS-1, SHC, and the IGF-IR. In MCF-7/IGF-IR cells, more IGF-IR appeared to be contained within E-cadherin complexes (Fig. 7). Interestingly, tyrosine phosphorylation of E-cadherin-associated SHC and IGF-IRs was not evidently increased in cells exposed to IGF-I for 48 h, whereas tyrosine phosphorylation of IRS-1 in the E-cadherin complex was quite prominent (Fig. 7). The molecular bases of this effect remain to be determined. It is possible that incorporation of the IGF-IR and SHC into adhesion complex accelerates dephosphorylation. IRS-1, resistant to this dephosphorylation, is probably a substrate of a different phosphatase(s).

In several experiments, we consistently observed an inhibitory effect of IGF-I on tyrosine phosphorylation of a 120-kDa protein whose position corresponded to that of E-cadherin (Fig. 7, MCF-7 cells, clone 12 and clone 15). Possibly, one of the functions of the IGF-IR in MCF-7 cells is to increase cell aggregation through dephosphorylation of E-cadherin. The interplay between growth factor- or oncoprotein-induced signaling and the regulation of cell-cell adhesion has already been described. For instance, EGF interferes with phosphorylation status of molecules engaged in adherens-type junctions, i.e., β -catenin is phosphorylated upon EGF stimulation [41]. In addition, expression of v-src causes tyrosine phosphorylation of E-cadherin and disrupts the cadherin-catenin complexes [42]. Cell-cell association can also be regulated by modification of the expression of adhesion proteins. For instance, overexpression of the ERB-B2 receptor or treatment with TGF- β inhibited expression of E-cadherin in normal mammary cells [43, 44]. In our model, there was no apparent modulation of E-cadherin expression.

Our experiments are still insufficient to resolve whether E-cadherin binds directly to either the IGF-IR or one of its substrates or if other intermediate proteins may be necessary to mediate this association. In fact, our preliminary data demonstrated that the IGF-IR is also present in β - and α -catenin precipitates. Similarly, since both IRS-1 and SHC can associate with the IGF-IR, binding of only one of those proteins to E-cadherin should be sufficient to form a multielement complex. Regardless of the nature of the association, the evident proximity of cell-cell adhesion molecules and the elements of IGF-IR signaling support our data implicating the IGF-IR in the regulation of epithelial aggregation.

The mechanism of IGF-IR-dependent cell-cell adhesion is currently unknown. The hypothesis that catalytic function of the receptor is involved is supported by the notion that in the presence of IGF-I, aggregation was induced and partial dephosphorylation of E-cadherin was observed. The other possibility is that the clusterization of receptors, due to activation by IGF-I or resulting from overexpression, induced concomitant

clusterization of associated E-cadherin complexes, which created stronger contacts and promoted aggregation.

In summary, our findings suggest a complex role of the IGF-IR in breast cancer. On one hand, increased levels of IGF-IRs induce hypersensitivity to IGF-I in the presence of E2, which may provide a growth advantage for cancer cells under conditions of low IGF-I availability (for example, in patients undergoing tamoxifen treatment [45]). On the other hand, the overexpression of the IGF-IR inhibits cell scattering, and, therefore, may have a role in the growth of noninvasive, differentiated breast tumors. The latter supports the data demonstrating that in breast cancer, higher levels of receptor predict better prognosis [11]. The "antiscattering" function of the IGF-IR, however, does not seem to be universal. In other systems (such as invasive lung carcinoma), this receptor is required for metastatic activity [46]. Unquestionably, more studies are required to define the role of IGF signaling in metastasis as well as in other neoplastic processes.

We are grateful to Drs. Renato Baserga, Gerald Grunwald, and Jerzy W. Kolaczynski for critically reading the manuscript and to David Dicker for his expert assistance with FACS analysis. This work was supported in part by NIH Grant DK48969 (E.S.). E.S. is a recipient of a Career Development Award TR950198 from the U.S. Army.

REFERENCES

1. Ullrich, A., Gray, A., Tam, A. W., Yang-Feng, T., Tsubokawa, M., Collins, C., Henzel, W., Le Bon, T., Kahuria, S., Chen, E., Jakobs, S., Francke, U., Ramachandran, J., and Fujita-Yamaguchi, Y. (1986) *EMBO J.* **5**, 2503-2512.
2. Myers, M. G., Sun, X. J., and White, M. F. (1994) *Trends Biochem. Sci.* **19**, 289-293.
3. Keller, S. R., and Lienhard, G. E. (1994) *Trends Cell Biol.* **4**, 115-119.
4. Giorgetti, S., Pelicci, P. G., Pelicci, G., and Van Obberghen, E. (1994) *Eur. J. Biochem.* **223**, 195-202.
5. Pelicci, G., Lanfrancone, L., Grignani, F., McGlade, J., Cavallo, F., Forni, G., Nicoletti, I., Grignani, F., Pawson, T., and Pelicci, P. G. (1992) *Cell* **70**, 93-104.
6. Vuori, K., and Ruoslahti, E. (1994) *Science* **266**, 1576-1578.
7. Spargaren, M., Bischoff, J. R., and McCormick, F. (1995) *Gene Expr.* **4**, 345-346.
8. Joneson, T., White, M. A., Wigler, M. H., and Bar-Sagi, D. (1996) *Science* **271**, 810-812.
9. Rubin, R., and Baserga, R. (1995) *Lab. Invest.* **73**, 311-331.
10. Ellis, M. J. C., Singer, C., Hornby, A., Rasmussen, A., and Culen, K. J. (1994) *Breast Cancer Res. Treat.* **31**, 249-261.
11. Papa, V., Gliozzo, B., Clark, G. M., McGuire, W. L., Moore, D., Fujita-Yamaguchi, Y., Vigneri, R., Goldfine, I. D., and Pezzino, V. (1993) *Cancer Res.* **53**, 3735-3740.
12. Rocha, R. L., Hilsenbeck, S. G., Jackson, J. G., and Yee, D. (1995) *Breast Cancer Res. Treat. Suppl.* **37**, 55.
13. Stewart, A. J., Johnson, M. D., May, F. E. B., and Westley, B. R. (1990) *J. Biol. Chem.* **265**, 21172-21178.

14. Surmacz, E., and Burgaud, J.-L. (1995) *Clin. Cancer Res.* **1**, 1429–1436.
15. Dickson, R. B., and Lippman, M. E. (1987) *Endocr. Rev.* **8**, 29–43.
16. Figueroa, J. A., and Yee, D. (1992) *Breast Cancer Res. Treat.* **22**, 81–90.
17. Cullen, K. J., Lippman, M. E., Chow, D., Hill, S., Rosen, N., and Zwiebel, J. A. (1992) *Mol. Endocrinol.* **6**, 91–100.
18. Arteaga, C. L., and Osborne, C. K. (1989) *Cancer Res.* **49**, 6237–6241.
19. Yee, D., Jackson, J. G., Kozelsky, T. W., and Figueroa, J. A. (1994) *Cell Growth Differ.* **5**, 73–77.
20. Neuenschwander, S., Roberts, C. T., Jr., and LeRoith, D. (1995) *Endocrinology* **136**, 4298–42303.
21. Guerra, F. K., Eijan, A. M., Puricelli, L., Alonso, D. E., Joffe, E. B. D., Kornblihtt, A. R., Charreau, E. H., and Elizalde, P. V. (1996) *Int. J. Cancer* **65**, 812–820.
22. Pantel, K., Schlimok, G., Angstwurm, M., Passlick, B., Izbicki, J. R., Johnson, J. P., and Riethmuller, G. (1995) in *Cell Adhesion and Human Disease*, Ciba Foundation Symposium 189, pp. 157–173, Wiley, Chichester.
23. Birchmeier, W., Hulsken, J., and Behrens, J. (1995) in *Cell Adhesion and Human Disease*, Ciba Foundation Symposium 189, pp. 124–141, Wiley, Chichester.
24. Birchmeier, W., Hulsken, J., and Behrens, J. (1995) *Cancer Surveys* **24**, 129–140.
25. Sommers, C., Gelmann, E. P., Kemler, R., Cowin, P., and Byers, S. W. (1994) *Cancer Res.* **54**, 3544–3552.
26. Bracke, M. E., Vyncke, B. M., Bruyneel, E. A., Vermeulen, S. J., De Bruyne, G. K., Van Larebeke, N. A., Vleminckx, K., Van Roy, F. M., and Mareel, M. M. (1993) *Br. J. Cancer* **68**, 282–289.
27. Bae, S.-N., Arand, G., Azzam, H., Pavasant, P., Torri, J., Frandsen, T. L., and Thompson, E. W. (1993) *Breast Cancer Res. Treat.* **24**, 241–255.
28. Vleminckx, K., Vakaet, L., Jr., Mareel, M., Fiers, W., and Van Roy, F. (1991) *Cell* **66**, 107–119.
29. Bracke, M. E., Charlier, C., Bruyneel, E. A., Labit, C., Mareel, M. M., and Castronovo, V. (1994) *Cancer Res.* **54**, 4607–4609.
30. Miura, M., Surmacz, E., Burgaud, J.-L., and Baserga, R. (1995) *J. Biol. Chem.* **270**, 22639–22644.
31. Soos, M. A., Whittaker, J., Lammers, R., Ullrich, A., and Siddle, K. (1990) *Biochem. J.* **270**, 383–390.
32. Zhou-Li, F., D'Ambrosio, C., Li, S., Surmacz, E., and Baserga, R. (1995) *Mol. Cell. Biol.* **15**, 4232–4239.
33. Goldstein, A., Aronow, L., and Kalman, S. M. (1974) in *Principles of Drug Action: The Basis of Pharmacology*, pp. 82–111, Wiley, Chichester.
34. Li, S., Ferber, A., Miura, M., and Baserga, R. (1994) *J. Biol. Chem.* **269**, 32558–32564.
35. Pietrzakowski, Z., Lammers, R., Carpenter, G., Soderquist, A., Limardo, M., Phillips, P., Ullrich, A., and Baserga, R. (1992) *Cell Growth Differ.* **3**, 199–205.
36. Daws, M. R., Westley, B. R., and May, F. E. B. (1996) *Endocrinology* **137**, 1177–1186.
37. Kleinman, D., Karas, M., Roberts, C. T., Jr., LeRoith, D., Philip, M., Sagev, Y., Levy, J., and Sharoni, Y. (1995) *Endocrinology* **136**, 2531–2537.
38. Miller, D. L., El-Ashry, D., Cheville, A. L., Liu, Y., McLeskey, S. W., and Kern, F. (1994) *Cell Growth Differ.* **5**, 1263–1274.
39. Liu, Y., El-Ashry, D., Chen, D., Yi Fan Ding, I., and Kern, F. G. (1995) *Breast Cancer Res. Treat.* **34**, 97–117.
40. Gelmann, E. P., Thompson, E. W., and Sommers, C. (1992) *Int. J. Cancer* **50**, 665–669.
41. Hoschuetzky, H., Aberle, H., and Kemler, R. (1994) *J. Cell Biol.* **127**, 1375–1380.
42. Behrens, J., Vakaet, L., Friis, R., Winterhager, E., Van Roy, F., Mareel, M. M., and Birchmeier, W. (1993) *J. Cell Biol.* **120**, 757–766.
43. D'Souza, B., and Taylor-Papadimitriou, J. (1994) *Proc. Natl. Acad. Sci. USA* **91**, 7202–7204.
44. Miettinen, P. J., Ebner, R., Lopez, A. R., and Derynck, R. (1994) *J. Cell Biol.* **127**, 2022–2036.
45. Colletti, R. B., Roberts, J. D., Devlin, J. T., and Copeland, K. C. (1989) *Cancer Res.* **49**, 1882–1884.
46. Long, L., Rubin, R., Baserga, R., and Brodt, P. (1995) *Cancer Res.* **55**, 1006–1009.

Received September 11, 1996

Revised version received November 25, 1996

Tamoxifen Interferes with the Insulin-like Growth Factor I Receptor (IGF-IR) Signaling Pathway in Breast Cancer Cells¹

Marina A. Guvakova and Ewa Surmacz²

Kimmel Cancer Institute, Thomas Jefferson University, Philadelphia, Pennsylvania 19107

Abstract

The insulin-like growth factor I receptor (IGF-IR) is involved in the control of breast cancer cell growth. The cytostatic activity of tamoxifen (Tam), a nonsteroidal antiestrogen, is partially mediated through interference with IGF-I-R-dependent proliferation, yet the effects of Tam on IGF-IR intracellular signaling have never been elucidated. Consequently, we investigated how Tam modifies the IGF-IR signaling pathway in estrogen receptor-positive MCF-7 breast cancer cells and in MCF-7-derived clones overexpressing either the IGF-IR (MCF-7/IGF-IR cells) or its major substrate, IRS-1 (MCF-7/IRS-1 cells). MCF-7/IGF-IR and MCF-7/IRS-1 cells exhibit greatly reduced estrogen growth requirements but retain estrogen receptors and express sensitivity to antiestrogens comparable to that in the parental cells. In all tested cell lines, regardless of the amplification of IGF signaling, a 4-day treatment with 10 nM Tam produced a similar cytostatic effect. In MCF-7 and MCF-7/IGF-IR cells, growth inhibition by Tam was associated with the reduced tyrosine phosphorylation of the IGF-IR in the presence of IGF-I; however, the basal level of the IGF-IR remained unaffected. Moreover, Tam inhibited both basal and IGF-I-induced tyrosine phosphorylation of IRS-1, which was accompanied by down-regulation of IRS-1-associated phosphatidylinositol 3'-kinase activity and reduced IRS-1/growth factor receptor-bound protein 2 (GRB2) binding. In contrast, under the same treatment, tyrosine phosphorylation of Src-homology/collagen proteins (SHC; another substrate of the IGF-IR) and SHC/GRB2 binding were elevated. The protein levels of the IGF-IR and IRS-1 were not modified by Tam, whereas SHC protein expression was either not affected or moderately decreased by the treatment.

In summary, this work provides the first evidence that in MCF-7 cells, cytostatic effects of Tam are associated with the modulation of IGF-IR signaling, specifically with: (a) down-regulation of IGF-I-induced tyrosine phosphorylation of the IGF-IR; (b) inhibition of IRS-1/phosphatidylinositol 3'-kinase signaling; and (c) up-regulation of SHC tyrosine phosphorylation and increased SHC/GRB2 binding. It is hypothesized that dephosphorylation of IRS-1 could be a major contributing factor in Tam cytostatic activity.

Introduction

The activation of the IGF-IR,³ through a paracrine, autocrine, or endocrine mechanism, appears to play a critical role in the regulation of breast cancer cell growth (1). The IGF-IR levels are significantly

higher in breast cancer than in normal breast tissue or benign tumors (1-3). The IGFs are potent mitogens for cultured breast cancer cells, and their expression has been documented in the epithelial and/or stromal component of breast tumors (1). In primary breast cancer, a correlation has been found between tumor size, the levels of IRS-1 (a cellular substrate of the IGF-IR), and recurrence of the disease (4). In MCF-7 breast cancer cells, the overexpression of either IRS-1 (5), the IGF-IR (6), or IGF-II (7) have been shown to reduce estrogen growth dependence. On the other hand, it has been demonstrated that blockade of IGF-IR signaling with, for instance, anti-IGF-IR antibodies (1), antisense RNA to the IGF-IR (8), and antisense oligodeoxynucleotides to IRS-1 (5) restricts breast cancer cell growth *in vitro* or *in vivo*.

The activation of the IGF-IR tyrosine kinase results in the stimulation of diverse intracellular pathways involving different signaling substrates (9). The best characterized substrates of the IGF-IR are IRS-1 and SHC. IRS-1 is a docking protein that, upon tyrosine phosphorylation by the IGF-IR, recruits several effector proteins through SH2-type interactions. For instance, IRS-1 binds and activates PI-3 kinase and SHC phosphatase as well as stimulates Ras/MAP pathway through the binding of GRB-2/SOS complexes (9). Moreover, IRS-1 has been found to interconnect with JAK-STAT (10) and integrin signaling pathways (11). SHC proteins are substrates of most tyrosine kinase receptors, many nonreceptor kinases and certain phosphatases (12, 13). Tyrosine phosphorylated SHC, similar to IRS-1, may activate Ras/MAP signaling cascade through the GRB2/SOS complex (12).

Tam, a nonsteroidal antiestrogen with partial agonist activity, is commonly used in adjuvant therapy in breast cancer management (14). Tam inhibits ER-dependent growth but also interferes with polypeptide growth factor signaling (14). The known effects of Tam or its derivative 4-OH-Tam on the IGF system in breast cancer cells include: inhibition of IGF-I stimulated growth (14, 15), modulation of IGFBP expression (1), reduced secretion of autocrine IGF (16), down-regulation of plasma levels of IGF-I in breast cancer patients (17), and decreased levels of IGF-I binding sites (18, 19). The interaction of Tam with the IGF-IR signaling pathway has not been characterized, partly because of the lack of adequate cellular models. Here, we investigated this aspect of Tam action using ER-positive MCF-7 cells as well as different MCF-7-derived cell lines overexpressing the elements of IGF-IR signaling.

Materials and Methods

Cell Lines and Cell Culture Conditions. MCF-7 cells were routinely grown in DMEM:F12 (1:1) containing 5% calf serum (6). In the experiments requiring estrogen-free conditions, the cells were cultured in phenol red-free DMEM containing 0.5 mg/ml BSA, 1 μ M FeSO₄ and 2 mM L-glutamine (PRF-SFM; Ref. 6).

MCF-7/IGF-IR, clones 12 and 15, and MCF-7/IRS-1, clone 3 were developed by stable transfection with the expression vectors pcDNA3/IGF-IR and CMV-IRS-1, respectively, and were characterized in detail previously (5, 6). The clones were maintained in culture for a maximum of 3 months in growth medium supplemented with 200 μ g/ml G418.

Received 3/7/97; accepted 5/13/97.

The costs of publication of this article were defrayed in part by the payment of page charges. This article must therefore be hereby marked *advertisement* in accordance with 18 U.S.C. Section 1734 solely to indicate this fact.

¹ This work was supported in part by Grant DK 48969 from the NIH (to E. S.). E. S. is a recipient of Career Development Award DAMD 17-96-1-6250 from the Department of the Army.

² To whom requests for reprints should be addressed, at Kimmel Cancer Institute BLSB 606A, Thomas Jefferson University, 233 South 10th Street, Philadelphia, PA 19107. Phone: (215) 503-4512; Fax: (215) 923-0249.

³ The abbreviations used are: IGF-IR, insulin-like growth factor I receptor; ER, estrogen receptor; GRB2, growth factor receptor-bound protein 2; IGFBP, IGF binding protein; IRS-1, insulin receptor substrate 1; MCF-7/IGF-IR, MCF-7 cells overexpressing IGF-IRs; MCF-7/IRS-1, MCF-7 cells overexpressing IRS-1; PI-3 kinase, phosphatidylinositol 3'-kinase; PRF-SFM, phenol red-free serum-free medium; SH2, src homology 2 domain; Tam, tamoxifen; SHC, Src-homology/collagen proteins; MAP, mitogen-activated protein kinase.

Cell Growth Assay. Cells (1×10^5) were plated in 24-well plates in DMEM:F12 (1:1) containing 5% calf serum. The next day, designed as day 0 of the experiment, the cells were shifted to either PRF-SFM or PRF-SFM supplemented with 0.1–100 nM Tam. For each cell line, the number of cells at day 0 was taken as 100% (control). The relative increase (percentage over control) in cell number was determined after 4 days of Tam treatment.

Western Blotting and Immunoprecipitation. The levels of the IGF-IR, IRS-1, SHC, as well as tyrosine phosphorylation of these proteins, were measured by Western blotting. The protein lysates (250–500 μ g) were obtained as described previously (6) and immunoprecipitated with the following antibodies: for IGF-IR, anti-IGF-IR monoclonal antibody alpha-IR3 (Oncogene Science); for IRS-1, anti-IRS-1 polyclonal antibody (UBI); and for SHC, anti-SHC polyclonal antibody (Transduction Laboratories). The immunoprecipitates were resolved by PAGE, and the IGF-IR, IRS-1, or SHC proteins were immunodetected with the following antibodies: for IRS-1, anti-IRS-1 polyclonal antibody (UBI); for IGF-IR and its M_r 200,000 precursor (20), anti-IGF-IR polyclonal antibody (Santa Cruz); and for SHC, anti-SHC monoclonal antibody (Transduction Laboratories). Tyrosine phosphorylation of the above proteins was detected by immunoblotting with an anti-phosphotyrosine monoclonal antibody PY20 (Transduction Laboratories). The intensity of bands was assessed by laser densitometry scanning.

PI-3 Kinase Activity. The activity of PI-3 kinase associated with IRS-1 was assessed by standard protocol provided by the manufacturer of the IRS-1 antibody (UBI). In brief, 500 μ g of protein lysate were immunoprecipitated with an anti-IRS-1 polyclonal antibody. The IRS-1 immunoprecipitates were incubated *in vitro* in the presence of 200 μ g/ml phosphatidylinositol (Sigma Chemical Co.) and 10 μ Ci [γ - 32 P]ATP for 30 min. The products of the kinase reaction were resolved on TLC plates (Eastman Kodak), and the spots corresponding to PI-3 phosphates were identified by autoradiography. The spots were then cut from the plates, and their radioactivity was counted with a beta counter. For each cell line, PI-3 kinase activity obtained in SFM was taken as 100% (control).

Results

Tam Inhibits the Growth of MCF-7 Breast Cancer Cells Overexpressing Either the IGF-IR or IRS-1. We studied whether Tam is able to inhibit the growth of MCF-7 cells with amplified IGF-IR signaling (MCF-7/IGF-IR and MCF-7/IRS-1 cells). The estrogen growth requirements in these cells are abolished or significantly reduced; however, the cells retain expression of the ER (5, 6). The effect of Tam on growth was studied in MCF-7/IGF-IR, clone 12 (expressing 5×10^5 IGF-I binding sites/cells; 8-fold IGF-IR overexpression over the levels in MCF-7 cells), MCF-7/IGF-IR, clone 15

(3×10^6 sites/cells; 50-fold IGF-IR overexpression), and in MCF-7/IRS-1, clone 3 (a 9-fold overexpression of IRS-1 over that in MCF-7 cells); MCF-7 cells were used as a control. The cells were cultured in PRF-SFM for 4 days in the presence of different concentrations of Tam (0.1–100 nM). Tam treatment suppressed growth of all cell lines in a dose-dependent manner (Fig. 1). Specifically, in all cells, 0.1, 1.0, and 10 nM Tam reduced proliferation by at least 12, 34, and 50%, respectively. The extent of Tam-induced growth inhibition in cells cultured for 4 days in PRF-SFM with 20 ng/ml IGF-I was comparable (data not shown). Treatment with 100 nM Tam was always cytotoxic. Consequently, Tam at a concentration of 10 nM was used in all further experiments.

Tam Interferes with IGF-I-induced Tyrosine Phosphorylation of the IGF-IR in MCF-7/IGF-IR Cells. To investigate the effects of Tam on IGF-IR signaling, we assessed tyrosine phosphorylation and protein levels of the IGF-IR in MCF-7 and MCF-7/IGF-IR, clone 15 cells. In cells cultured in PRF-SFM plus IGF-I, the IGF-IR tyrosine phosphorylation was always elevated compared with that in PRF-SFM (Fig. 2). After 4 days of treatment, the effects of Tam on the basal level of IGF-IR tyrosine phosphorylation were minimal (Fig. 2A); specifically, in several experiments either no modification or slight ($\sim 15\%$) up- or down-regulation were noticeable. However, Tam reduced IGF-I-induced tyrosine phosphorylation by 60% in MCF-7 cells and by 30% in MCF-7/IGF-IR cells (Fig. 2B).

The IGF-IR protein levels were not significantly modulated by Tam, as determined by laser densitometry scanning (Fig. 2). Similarly, the levels of the IGF-IR precursor were not affected by the treatment (Fig. 2A).

Inhibition of Cell Growth by Tamoxifen Is Associated with Dephosphorylation of IRS-1. In all tested cell lines, but especially in the clones with amplified IGF-IR signaling (MCF-7/IGF-IR, clones 12 and 15, and in MCF-7/IRS-1 cells), a basal level of IRS-1 tyrosine phosphorylation was evident even after prolonged culture in PRF-SFM, which reflected cellular response to autocrine IGFs, as shown previously (Refs. 5 and 6; Fig. 3, A and B). The addition of 10 nM Tam to PRF-SFM produced a cytostatic effect (Fig. 1), which was accompanied by a marked dephosphorylation of IRS-1 on tyrosine residues in the cells studied. Specifically, the basal level of IRS-1 tyrosine phosphorylation was reduced by 29, 35, and 48% in MCF-7/IGF-IR, clone 12, MCF-7/IGF-IR, clone 15, and MCF-7/IRS-1 cells, respectively (Fig. 3A). In MCF-7 cells, due to a low basal level of IRS-1

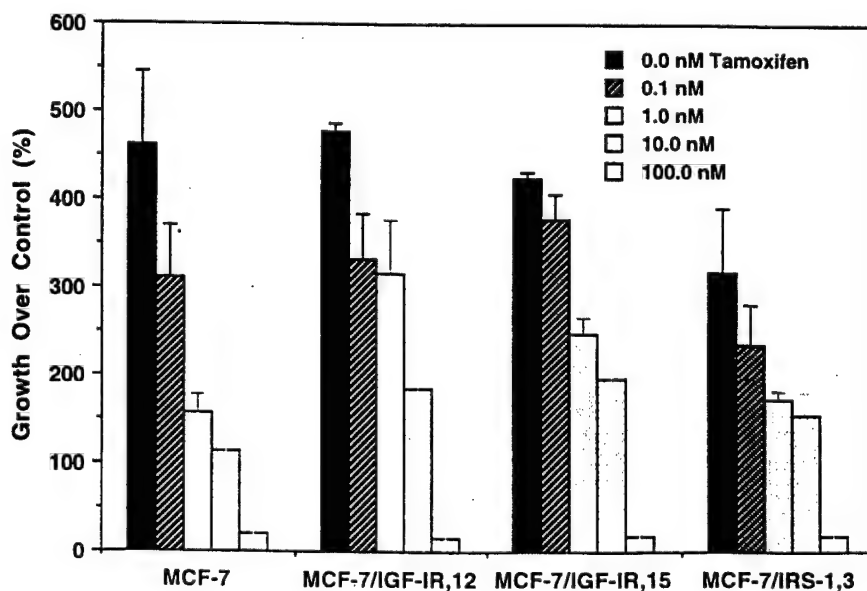


Fig. 1. Tam inhibits the growth of MCF-7 cells overexpressing either the IGF-IR or IRS-1. The cells were treated as described in "Materials and Methods." The results represent the percentage of growth inhibition relative to control (100%) in PRF-SFM. The results are means from at least four experiments. Bars, SE.

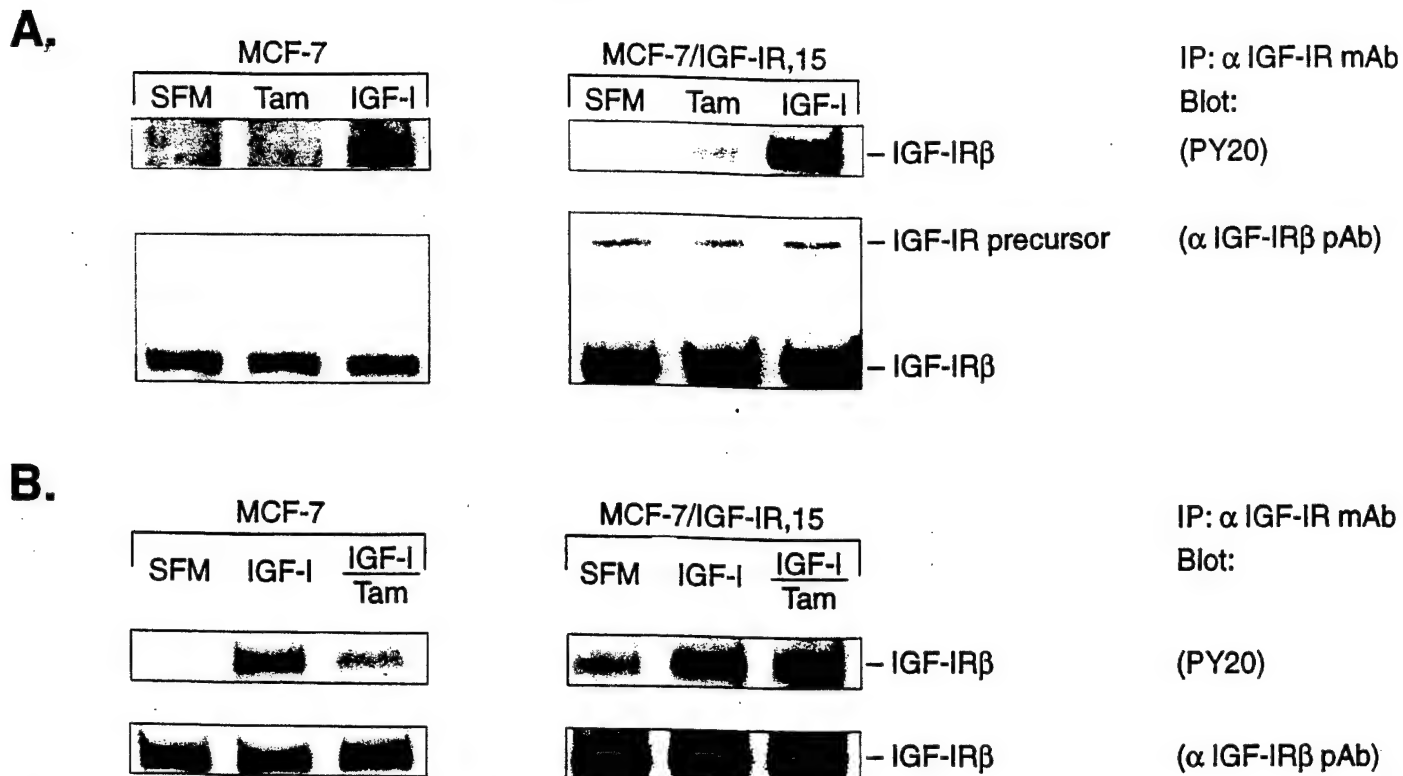


Fig. 2. Effects of Tam on the IGF-IR. **A.** Tam effect on basal level of IGF-IR tyrosine phosphorylation. The cells were lysed after 3 days of incubation in either PRF-SFM (SFM), PRF-SFM plus 10 nM Tam (Tam), or PRF-SFM plus 50 ng/ml IGF-I (IGF-I). Tyrosine phosphorylation and protein level of the IGF-IR were determined after immunoprecipitation of 500 μ g of protein lysates with an anti-IGF-IR monoclonal antibody followed by Western blotting with the indicated antibodies. **B.** Tam blocks IGF-I-induced tyrosine phosphorylation of the IGF-IR. Lane IGF-I/Tam, cells were cultured in PRF-SFM with 50 ng/ml IGF-I and 10 nM Tam; other conditions were as described for A. Representative results from four experiments are shown.

phosphorylation, the effect of Tam was not measurable. The interference of Tam with IRS-1 signaling was further studied in MCF-7/IRS-1 cells (Fig. 3B). The IGF-I-stimulated and basal levels of IRS-1 phosphorylation were suppressed in the presence of the drug by approximately 43% (Fig. 3B). The dephosphorylation of IRS-1 was accompanied by its dissociation from both p85 subunit of PI-3 kinase and GRB2 (Fig. 3B). Similar effects of Tam on IRS-1 tyrosine phosphorylation (approximately 27% inhibition) were seen in MCF-7/IGF-IR, clone 15 cells (data not shown).

In addition, Tam suppressed the activity of IRS-1-associated PI-3 kinase in cells stimulated with IGF-I; the inhibition by 43, 92, and 128% was seen in MCF-7, MCF-7/IGF-IR, and MCF-7/IRS-1, respectively (Fig. 3C). The effects of Tam on PI-3 kinase in cells cultured in PRF-SFM were not measurable.

In several repeat experiments, IRS-1 protein levels were not affected by long-term treatment with Tam (Fig. 3, A and B).

Tamoxifen Increases Tyrosine Phosphorylation of SHC. Of note, in all studied cell lines the cytostatic action of Tam was associated with the elevated tyrosine phosphorylation of p52^{SHC} and p46^{SHC} (Fig. 4). The activation of p52^{SHC} was especially prominent; specifically, compared with SHC status in untreated cells, a 34, 110, and 100% augmentation of p52^{SHC} tyrosine phosphorylation was observed in MCF-7, MCF-7/IGF-IR, and MCF-7/IRS-1 cells, respectively. Moreover, the hyperphosphorylation of p52^{SHC} was followed by an its increased binding to GRB2 (Fig. 4).

In contrast, in all cell lines, a 4-day exposure to IGF-I decreased tyrosine phosphorylation of p52^{SHC} by approximately 40% compared with that in PRF-SFM and induced dissociation of SHC/GRB2 complexes (Fig. 4).

Tam treatment produced a consistent down-regulation of p52^{SHC} and p46^{SHC} levels by approximately 35% in MCF-7/IGF-IR, clone 15

and MCF-7/IRS-1 cells but not in MCF-7 cells (Fig. 4). In contrast, SHC protein expression was not modulated by IGF-I (Fig. 4).

Effect of Tamoxifen on ERK2. Because IRS-1 and SHC, via GRB2/SOS, may activate Ras/MAP signaling pathway, we assessed MAP (ERK2) kinase activity in cells exposed to Tam or cultured for 4 days in PRF-SFM in the presence or absence of exogenous IGF-I. We found no differences in ERK2 activity under these conditions, measured in an *in vitro* assay, using myelin basic protein as a substrate (data not shown).

Discussion

Experimental evidence suggests an important role of the IGF-R in the pathobiology of breast tumors (1–3). Activation of the IGF-IR promotes proliferation and transformation as well as cell-cell and cell-substrate interactions in breast cancer cells (1, 5, 6, 21). Conversely, the blockade of IGF signaling results in the inhibition of breast cancer growth (1, 5, 8). Tam, or its derivative 4-OH-Tam, have been shown to inhibit IGF-IR-dependent growth through different mechanisms, such as down-regulation of autocrine IGF secretion (16) or modulation of IGF-BPs expression (1). In addition, in MCF-7 breast cancer cells, Tam and 4-OH-Tam decreased expression of IGF-I binding sites by approximately 30% (19) and 60% (18), respectively.

The effects of Tam on the IGF signal transduction pathway are unknown. Here, we report for the first time the modulation of the IGF-IR intracellular signaling pathways associated with the cytostatic action of Tam. Our studies focused on tyrosine kinase activity and protein levels of the IGF-IR and its two major cellular substrates, IRS-1 and SHC. Preliminary data from Rocha *et al.* (4) documented that IRS-1 is expressed in primary breast tumors and its levels correlate with increased recurrence. The status of SHC and its relation with

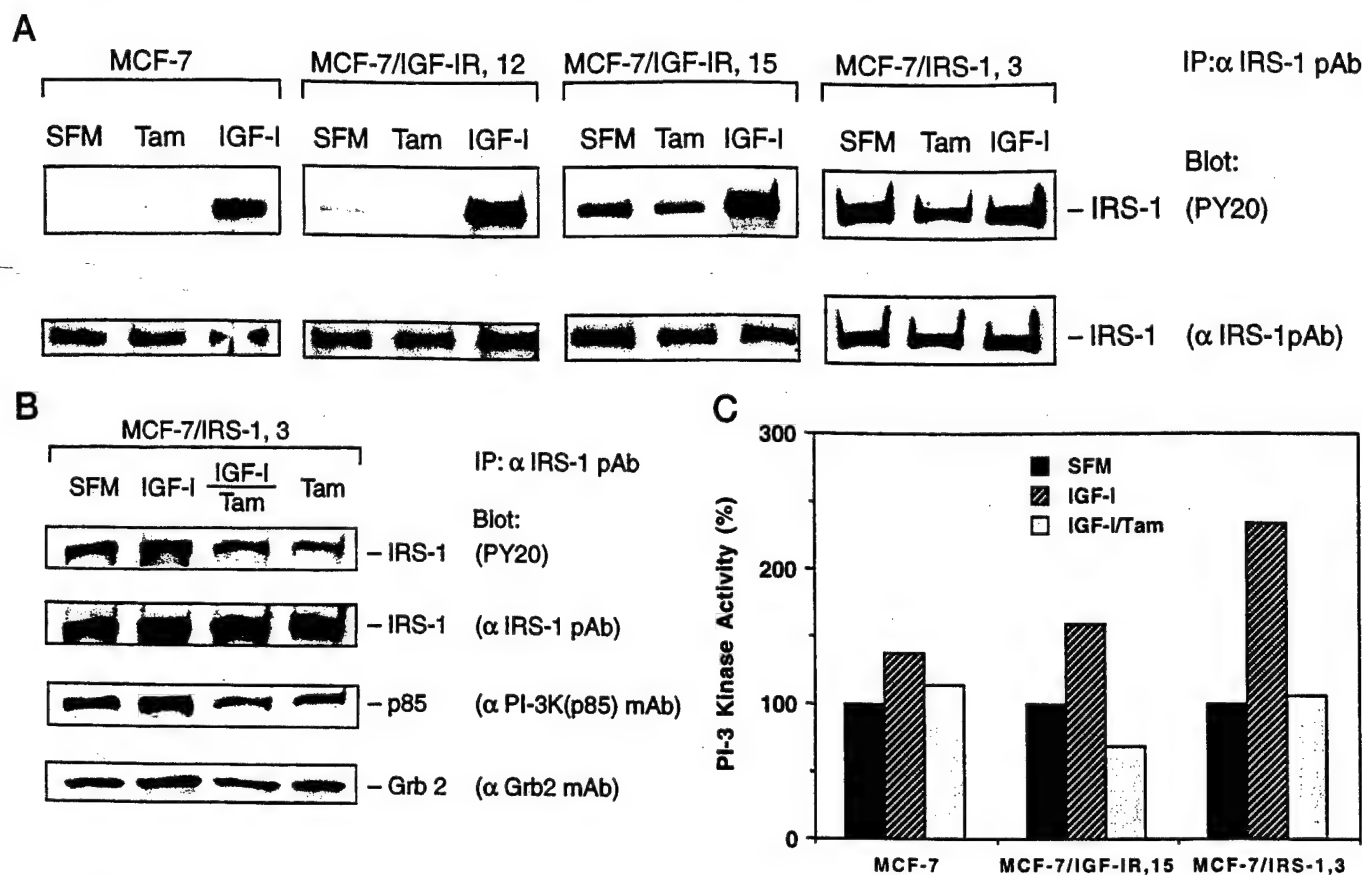


Fig. 3. Effects of Tam on IRS-1-mediated signaling. **A**, effects of Tam on IRS-1 tyrosine phosphorylation. MCF-7 cells, MCF-7/IGF-IR, clones 12 and 15, and MCF-7/IRS-1, clone 3, were incubated in PRF-SFM (SFM), PRF-SFM plus 10 nM Tam (Tam), or PRF-SFM plus 50 ng/ml IGF-I (IGF-I) for 3 days. IRS-1 was immunoprecipitated from 300 μ g of protein lysates, and tyrosine phosphorylation levels were detected with PY-20 antibody. IRS-1 protein level was determined in the original blot, after stripping and reprobing with an anti-IRS-1 antibody. Representative results from five experiments are shown. **B**, effects of Tam on IRS-1 signaling in MCF-7/IRS-1 cells. MCF-7/IRS-1, clone 3, was cultured for 4 days in either PRF-SFM (SFM), PRF-SFM plus 50 ng/ml IGF-I alone (IGF-I), PRF-SFM plus 50 ng/ml IGF-I with 10 nM Tam (IGF-I/Tam), or PRF-SFM plus 10 nM Tam (Tam). IRS-1 was immunoprecipitated from 250 μ g of lysates, and IRS-1 protein level and tyrosine phosphorylation were detected as described above. Amounts of p85 of PI-3 kinase and GRB2 associated with IRS were determined in original nitrocellulose filters after stripping and reprobing with specific antibodies. **C**, Tam effects on IRS-1 associated PI-3 kinase activity. The cells were incubated in PRF-SFM (SFM), PRF-SFM plus 50 ng/ml IGF-I (IGF-I), or PRF-SFM plus 50 ng/ml IGF-I and 10 nM Tam (IGF-I/Tam) for 3 days. IRS-1 was precipitated from 500 μ g of cell lysates from each cell line. The activity of PI-3 kinase associated with IRS-1 was assessed *in vitro* as described in "Materials and Methods." The results are expressed as percentage of increase over control levels in SFM (100%). Representative data are shown.

different prognostic markers is not known. Our experiments with MCF-7 cells expressing antisense RNA to either IRS-1 or SHC demonstrated that normal levels of both substrates are critical in sustaining monolayer and anchorage-independent growth.⁴ In addition, IRS-1 signaling appears to play a role in the protection from apoptosis *in vitro*.⁴

Here, we looked at the status of IRS-1 and SHC in the state of growth inhibition induced by Tam. We approached this problem using MCF-7 cells as well as more sensitive cellular models, *i.e.*, MCF-7-derived clones overexpressing either the IGF-IR or IRS-1 (5, 6). The amplification of IGF-IR signaling in MCF-7 cells promotes growth responsiveness to IGF-I and abrogates estrogen growth requirements but does not influence ER expression and function (5, 6). In this work, we demonstrated that estrogen independence in MCF-7/IGF-IR and MCF-7/IRS-1 cells does not circumvent sensitivity to cytostatic action of Tam. Remarkably, the inhibition of growth was similar in all studied cell lines, regardless of the amplification of IGF-IR signaling. With this experimental system we have made several important observations:

(a) Tam had no apparent effect on IGF-IR protein levels or the levels of its precursor, at least in a 4-day experiment. Other studies

demonstrated a small (30%) down-regulation of IGF binding sites in Tam-treated MCF-7 cells (19); however, binding assays were performed without discriminating IGF-I association with membrane IGF-BPs, which could result in miscalculation of IGF-IR levels (22).

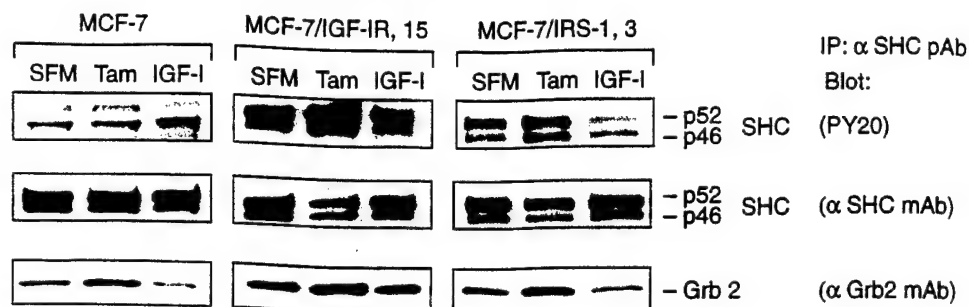
(b) Tam inhibited IGF-I-induced tyrosine phosphorylation of the IGF-IR. It is unlikely that this effect was mediated exclusively through the reduction of the amount of autocrine IGFs because Tam effectively suppressed autocrine growth without modification of the basal IGF-IR tyrosine phosphorylation (in PRF-SFM; Figs. 1 and 2). Why the effect of Tam on IGF-IR activation is evident in the presence of excess IGF-I but not with autocrine IGFs remains to be clarified; possibly, the regulation of the phosphatase system is different under these two conditions. This observation, however, suggests that continuing dephosphorylation of the IGF-IR is not critical for Tam-induced growth arrest.

(c) Tam treatment resulted in the persisting dephosphorylation of IRS-1 on tyrosine residues, apparently in the presence of both autocrine and exogenous IGF-I. The attenuation of IRS-1 tyrosine phosphorylation by Tam was accompanied by down-regulation of IRS-1-associated PI-3 kinase activity and dissociation of GRB2 from IRS-1. Our findings agree with preliminary data of Kleinman *et al.* (23), who demonstrated that Tam inhibited tyrosine phosphorylation of a M_r 185,000 protein (possibly IRS-1) in MCF-7 cells.

(d) The effect of Tam on SHC was evidently different from that seen

⁴ M. Nolan, L. Jankowska, M. Prisco, S. Xu, M. Guvakova, and E. Surmacz. Differential roles of IRS-1 and SHC signaling pathways in breast cancer cells. *Int. J. Cancer*, in press.

Fig. 4. Effects of Tam on SHC signaling. The cells were grown in either PRF-SFM (SFM), PRF-SFM plus 10 nM Tam (Tam), or PRF-SFM plus 50 ng/ml IGF-I (IGF-I) for 3 days. SHC protein were immunoprecipitated from 500 μ g of cell lysates with an anti-SHC polyclonal antibody followed by detection of tyrosine phosphorylation of SHC with PY-20. The SHC protein and SHC-associated GRB2 were detected in original filters, upon stripping and re-probing with specific antibodies. Representative results of five experiments are shown.



for IRS-1. Here, growth inhibition was associated with elevated tyrosine phosphorylation of SHC proteins, especially p52^{SHC}, without up-regulation of SHC protein levels. Importantly, long-term treatment with IGF-I, which promoted growth, concomitantly reduced SHC phosphorylation. Whether up-regulation of SHC phosphorylation is a universal feature of growth arrest or it only represents a characteristic of Tam action is presently unclear. In MCF-7 cells, treatment with genistein or herbimycin inhibited proliferation, which was associated with a reduction of SHC tyrosine phosphorylation observed after 30 min treatment (24). Longer effects of these tyrosine kinase inhibitors were not studied. In our system, higher phosphorylation of SHC in Tam-treated cells was accompanied by GRB2 binding to SHC; however, activation of ERK2 was not observed. Possibly, under Tam treatment, activation of ERK2 via SHC was counteracted by deactivation of this pathway due to disruption of IRS-1 signaling. Alternatively, as suggested by others (24, 25), the ERK2 pathway is not critical in IGF-stimulated growth in MCF-7 cells; thus, it is not a target for Tam action.

In summary, these results demonstrate that Tam differentially modulates IGF-IR signaling in breast cancer cells. The cytostatic effect of Tam is mediated by a continuing inhibition of IRS-1/PI-3 kinase pathway. On the other hand, Tam increases tyrosine phosphorylation of SHC and SHC/GRB2 binding. The biological consequences of the latter effects are presently unknown.

One possible target of Tam action is the tyrosine phosphatase system. Indeed, Freiss and Vignon (26) have recently shown that 4-hydroxytamoxifen up-regulates protein tyrosine phosphatase activity in breast cancer cells. We speculate that Tam activates, most probably through an indirect mechanism, a specific tyrosine phosphatase(s) acting upon IRS-1. On the other hand, Tam may also inhibit tyrosine phosphatase(s) that would specifically affect SHC and/or the IGF-IR. Future experiments with Tam and pure antiestrogens will further explore this issue, especially in relation with such phenomenon as antiestrogen resistance or Tam-induced growth.

References

- Lee, A. V., and Yee, D. Insulin-like growth factors and breast cancer. *Biomed. Pharmacother.*, **49**: 415–421, 1995.
- Papa, V., Gliozzo, B., Clark, G. M., McGuire, W. L., Moore, D., Fujita-Yamaguchi, Y., Vigneri, R., Goldfine, I. D., and Pezzino, V. Insulin-like growth factor I receptors are overexpressed and predict a low risk in human breast cancer. *Cancer Res.*, **53**: 3735–3740, 1993.
- Peyrat, J. P., and Bonnetterre, J. Type I IGF receptor in human breast diseases. *Breast Cancer Res. Treat.*, **22**: 59–68, 1992.
- Rocha, R. L., Hilsenbeck, S. G., Jackson, J. G., and Yee, D. Insulin-like growth factor binding protein-3 (IGFBP3) and insulin receptor substrate (IRS1) in primary breast cancer: larger tumors have higher BP3 levels and higher levels of IRS-1 are associated with lower disease-free survival (DFS) rate. *Breast Cancer Res. Treat.* **37**(Suppl.): 55, 1995.
- Surmacz, E., and Burgaud, J.-L. Overexpression of insulin receptor substrate 1 (IRS-1) in the human breast cancer cell line MCF-7 induces loss of estrogen requirements for growth and transformation. *Clin. Cancer Res.*, **1**: 1429–1436, 1995.
- Guvakova, M. A., and Surmacz, E. Overexpressed IGF-I receptors reduce estrogen growth requirements, enhance survival, and promote E-cadherin-mediated cell-cell adhesion in human breast cancer cells. *Exp. Cell. Res.*, **149**–162, 1997.
- Cullen, K. J., Lippman, M. E., Chow, D., Hill, S., Rosen, N., and Zwiebel, J. A. Insulin-like growth factor-II overexpression in MCF-7 cells induces phenotypic changes associated with malignant progression. *Mol. Endocrinol.*, **6**: 91–100, 1992.
- Neuenschwander, S., Roberts, C. T., Jr., and LeRoith, D. Growth inhibition of MCF-7 breast cancer cells by stable expression of an insulin-like growth factor I receptor antisense ribonucleic acid. *Endocrinology*, **136**: 4298–4303, 1995.
- Rubin, R., and Baserga, R. Biology of disease. Insulin-like growth factor-I receptor. Its role in cell proliferation, apoptosis and tumorigenicity. *Lab. Invest.*, **73**: 311–331, 1995.
- Argetsinger, L. S., Hsu, G. W., Myers, M. G., Billestrup, N., White, M. F., and Carter-Su, C. Growth hormone, interferon- γ , and leukemia inhibitory factor promoted tyrosyl phosphorylation of IRS-1. *J. Biol. Chem.*, **270**: 14685–14692, 1995.
- Vuori, K., and Ruoslahti, E. Association of insulin receptor substrate-1 with integrins. *Science (Washington DC)*, **266**: 1576–1578, 1994.
- Pellicci, G., Lanfrancone, L., Salcini, A. E., Romano, A., Mele, S., Borrello, M. G., Segatto, O., Di Fiore, P. P., and Pellicci, P. G. Constitutive phosphorylation of Shc proteins in human cancers. *Oncogene*, **11**: 899–907, 1995.
- Habib, T., Herrera, R., and Decker, S. J. Activators of protein kinase C stimulate association of Shc and the PEST tyrosine phosphatase. *J. Biol. Chem.*, **269**: 25243–25246, 1994.
- Jordan, C. V. Molecular mechanisms of antiestrogen action in breast cancer. *Breast Cancer Res. Treat.*, **31**: 41–52, 1994.
- de Cupis, A., Noonan, D., Pirani, P., Ferrera, A., Clerico, L., and Favoni, R. E. Comparison between novel steroid-like and conventional nonsteroidal antiestrogens in inhibiting oestradiol- and IGF-I-induced proliferation of human breast cancer-derived cells. *Br. J. Pharmacol.*, **116**: 2391–2400, 1995.
- Huff, K. K., Knabbe, C., Linsey, R., Kaufman, D., Bronzert, D., Lippman, M. E., and Dickson, R. B. Multihormonal regulation of insulin-like growth factor-I-related protein in MCF-7 cells. *Mol. Endocrinol.*, **2**: 200–208, 1988.
- Colletti, R. B., Roberts, J. D., Devlin, J. T., and Copeland, K. C. Effect of tamoxifen on plasma insulin-like growth factor I in patients with breast cancer. *Cancer Res.*, **49**: 1882–1884, 1989.
- Freiss, G., Rochefort, H., and Vignon, F. Mechanisms of 4-hydroxytamoxifen anti-growth factor activity in breast cancer cells: alterations of growth factor receptor binding sites and tyrosine kinase activity. *Biochem. Biophys. Res. Commun.*, **173**: 919–926, 1990.
- Kawamura, I., Lacey, E., Mizota, T., Tsuimoto, S., Nishigaki, F., Manda, T., and Shimomura, K. The effect of droloxifene on the insulin-like growth factor-I-stimulated growth of breast cancer cells. *Anticancer Res.*, **14**: 427–432, 1994.
- Yamasaki, H., Prager, D., Gebremedhin, S., and Melmed, S. Insulin-like growth factor-I (IGF-I) attenuation of growth hormone is enhanced by overexpression of pituitary IGF-I receptors. *Mol. Endocrinol.*, **5**: 890–896, 1991.
- Doerr, M., and Jones, J. The roles of integrins and extracellular matrix proteins in the IGF-I-stimulated chemotaxis of human breast cancer cells. *J. Biol. Chem.*, **271**: 2443–2447, 1996.
- Kleinman, D., Karas, M., Roberts, C. T., Jr., LeRoith, D., Phillip, M., Segev, Y., Levy, J., and Sharoni, Y. Modulation of insulin-like growth factor I receptors and membrane-associated IGF-I binding proteins in endometrial cancer cells by estradiol. *Endocrinology*, **136**: 2531–2537, 1995.
- Kleinman, D., Karas, M., Danilenko, M., Arbeli, A., Roberts, C. T., Jr., LeRoith, D., Levy, J., and Sharoni, Y. Stimulation of endometrial cancer cell growth by tamoxifen is associated with increased insulin-like growth factor (IGF)-I induced tyrosine phosphorylation and reduction in IGF binding proteins. *Endocrinology*, **137**: 1089–1095, 1996.
- Clark, J. W., Santos-Moore, A., Stevenson, L. E., and Frackelton, A. R., Jr. Effects of tyrosine kinase inhibitors on the proliferation of human breast cancer cell lines and proteins important in the ras signaling pathway. *Int. J. Cancer*, **65**: 186–191, 1996.
- Vinkvanwijngaarden, T., Pols, H. A. P., Buurman, C. J., Birkenhager, J. C., and Vanleeuwen, J. P. T. M. Inhibition of insulin- and insulin-like growth factor-I-stimulated growth of human breast cancer cells by 1,25-dihydroxyvitamin D-3 and the vitamin D-3 analogue EB 1089. *Eur. J. Cancer*, **32A**: 842–848, 1996.
- Freiss, G., and Vignon, F. Antiestrogens increase protein tyrosine phosphatase activity in human breast cancer cells. *Mol. Endocrinol.*, **8**: 1389–1396, 1994.

INSULIN RECEPTOR SUBSTRATE 1 (IRS-1) IS A TARGET FOR A PURE ANTIESTROGEN ICI 182,780 IN BREAST CANCER CELLS

Michele SALERNO^{§¥}, Diego SISCO^{§¥}, Loredana MAURO^{§¥}, Marina A.
GUVAKOVA[§], Sebastiano ANDÒ[¥] and Ewa SURMACZ^{§1}

[§]Kimmel Cancer Center, Thomas Jefferson University, Philadelphia PA 19107 and

[¥]Department of Cellular Biology, University of Calabria, Cosenza, Italy

Running title: ICI 182,780 downregulates IRS-1

Key words: ICI 182,780; IRS-1; antiestrogen resistance; IGF-I; breast cancer

¹Corresponding author:

Ewa Surmacz, Ph.D.
Kimmel Cancer Center
Thomas Jefferson University
233 S. 10th Street, BLSB 606
Philadelphia, PA 19107
tel. 215-503-4512
FAX 215-923-0249
e-mail: surmacz1@jefflin.tju.edu

ABSTRACT

The pure antiestrogen ICI 182,780 inhibits insulin-like growth factor (IGF)-dependent proliferation in hormone-responsive breast cancer cells. However, the interactions of ICI 182,780 with IGF-I receptor (IGF-IR) intracellular signaling have not been characterized. Here, we studied the effects of ICI 182,780 on IGF-IR signal transduction in MCF-7 breast cancer cells and in MCF-7-derived clones overexpressing either the IGF-IR, or its two major substrates: IRS-1 (insulin receptor substrate 1) or SHC (src/collagen homology proteins).

ICI 182,780 blocked the basal and IGF-I-induced growth in all studied cells in a dose-dependent manner, however, the clones with the greatest IRS-1 overexpression were clearly least sensitive to the drug. Pursuing ICI 182,780 interaction with IRS-1, we found that the antiestrogen reduced IRS-1 expression and tyrosine phosphorylation in several cell lines in the presence or absence of IGF-I. Moreover, in IRS-1-overexpressing cells, ICI 182,780 decreased IRS-1/p85 and IRS-1/GRB2 binding.

The effects of ICI 182,780 on IGF-IR protein expression were not significant, however the drug suppressed IGF-I-induced (but not basal) IGF-IR tyrosine phosphorylation. The expression and tyrosine phosphorylation of SHC as well as SHC/GRB binding were not influenced by ICI 182, 780.

In summary, downregulation of IRS-1 may represent one of the mechanisms by which ICI 182,780 inhibits the growth of breast cancer cells. Thus, overexpression of IRS-1 in breast tumors could contribute to the development of antiestrogen resistance.

INTRODUCTION

ICI 182,780, an alpha-alkylsulphinyamide, is a new generation pure antiestrogen that has shown a great promise as a second line endocrine therapy agent in patients with advanced breast cancer resistant to the non-steroidal antiestrogen Tamoxifen (Tam) (1-5). In several in vitro and in vivo studies, the anti-tumor effects of ICI 182,780 were greater than that of Tam (1-6). Moreover, unlike Tam, ICI 182,780 lacks agonist (estrogenic) activity and its administration does not appear to be associated with deleterious site effects such as induction of endometrial cancer or retinopathy (4). ICI 182,780 antagonizes multiple cellular effects of estrogens by impairing the dimerization of the estrogen receptor (ER) and by reducing ER half-life (3, 4). ICI 182,780 also interferes with growth factor-induced growth, but it is not clear if this activity is mediated exclusively through the ER, or some ER-independent mechanism is implicated (6). Despite their great antitumor effects, pure antiestrogens do not circumvent the development of antiestrogen-resistance, as most breast tumor cells initially sensitive to ICI 182,780 eventually become unresponsive to the drug (3, 4, 7, 8). The mechanism of this resistance is not clear, but it has been suggested that both mutations of the ER as well as alterations in growth factor-dependent mitogenic pathways may be involved (3, 8-10).

The IGF system (IGFs, the IGF-IR, and IGF binding proteins (IGFBP)) plays a critical role in the pathobiology of hormone-responsive breast cancer (11-13). In the experimental setting, the IGF-IR has been shown to stimulate growth and transformation, improve survival as well as regulate cell-cell and cell-substrate interactions in breast cancer cells (11, 12, 14-19). Moreover, overexpression of different elements of the IGF system, such as IGF-II, the IGF-IR or IRS-1, provides breast cancer cells with growth advantage and reduces or abrogates estrogen growth requirements (15, 20, 21). On the other hand, downregulation of IGF-IR expression, inhibition of IGF-IR signaling, or reduced bioavailability of the IGFs have been demonstrated to block proliferation and survival as

well as interfere with motility or intercellular adhesion in breast cancer cells (11, 12, 14-19).

Clinical studies confirm the role of the IGF-I system in breast cancer development. First, the IGF-IR has been found up to 14-fold overexpressed in breast cancer compared with its levels in normal mammary epithelium (22-24). Moreover, cellular levels of the IGF-IR or its substrate IRS-1 correlate with cancer recurrence at the primary site (25, 26). The ligands of the IGF-IR, IGF-I and IGF-II, are often present in the epithelial and/or stromal component of breast tumors indicating that an autocrine or a paracrine IGF-IR loop may be operative and involved in the neoplastic process (11, 27). In addition, endocrine IGFs probably also contribute to breast tumorigenesis since the levels of circulating IGF-I correlate with breast cancer risk in premenopausal women (28).

ICI 182,780 interferes with the IGF-I system in breast cancer cells. The antiestrogen has been shown to attenuate IGF-I stimulated growth (6), modulate expression of IGFBPs (18, 19) and downregulate IGF binding sites (3). The interactions of ICI 182,780 with the IGF-IR signaling pathways, however, have not been characterized.

Our previous work demonstrated that in breast cancer cells, Tam interferes with the IGF-IR signaling acting upon IGF-IR substrates IRS-1 and SHC (29). Normally, activation of the IGF-IR results in the recruitment and tyrosine phosphorylation of IRS-1 and SHC, followed by their association with several downstream effector proteins and induction of various signaling pathways (12, 13, 30). For instance, association of either IRS-1 or SHC with GRB-2/SOS complexes activates Ras/MAP pathway, whereas binding of IRS-1 with p85 stimulates PI-3 kinase (13, 30). Tam treatment blocks IGF-dependent growth, which coincides with decreased tyrosine phosphorylation of IRS-1 and the IGF-IR and with hyperphosphorylation of SHC (29). Here, we demonstrate the interactions of ICI 182,780 with IGF-IR signaling and discuss the relevant similarities and differences in the modes of action of the two antiestrogens.

MATERIALS AND METHODS

Cell Lines and Cell Culture Conditions. In this study we used MCF-7 cells and several MCF-7-derived clones overexpressing either the IGF-IR (MCF-7/IGF-IR cells), IRS-1 (MCF-7/IRS-1 cells) or SHC (MCF-7/SHC cells). MCF-7/IGF-IR, clone 17 and MCF-7/IRS-1 clones 9, 3 and 18 were developed by stable transfection of MCF-7 cells with expression vectors encoding either the IGF-IR or IRS-1 and were characterized previously (15, 21). MCF-7/SHC cells are MCF-7-derived cells transfected with the plasmid pcDNA3/SHC; compared with MCF-7 cells, the level of p55^{SHC} and p47^{SHC} overexpression in MCF-7/SHC cells is approximately 5-fold (manuscript submitted)³. The above MCF-7-derived clones express ERs and respond to E2, similar to MCF-7 cells (15, 21). The levels of IRS-1 in MCF-7/IGF-IR and MCF-7/SHC cells are similar to those in MCF-7 cells (Fig. 2B and unpublished results).

MCF-7 cells were grown in DMEM:F12 (1:1) containing 5% calf serum (CS). MCF-7-derived clones were maintained in DMEM:F12 plus 5% CS plus 200 ug/ml G418 (15, 21). In the experiments requiring E2-free conditions, the cells were cultured in phenol red-free DMEM containing 0.5 mg/ml BSA, 1 uM FeSO₄ and 2 mM L-glutamine (PRF-SFM) (15, 17).

Cell Growth Assay. Cells were plated at a concentration 2×10^5 in 6-well plates in a growth medium; the following day (day 0), the cells were shifted to PRF-SFM containing different doses of ICI 182,780 (1-300 nM) with or without 50 ng/ml IGF-I and incubated for 4 days. The increase in cell number from day 0 to day 4 in PRF-SFM was designated as 100 % growth increase.

Immunoprecipitation and Western Blotting. The expression and tyrosine phosphorylation of IGF-I signaling proteins were measured by immunoprecipitation (IP) and Western blotting (WB), as described before (15, 21). Protein lysates (500 ug) were immunoprecipitated with the following antibodies (Abs): for the IGF-IR: anti-IGF-IR monoclonal Ab (mAb) alpha-IR3 (Oncogene Science); for IRS-1: anti-C-terminal IRS-1

polyclonal Ab (pAb) (UBI); for SHC: anti-SHC pAb (Transduction Laboratories). Tyrosine phosphorylation was probed by WB with an anti-phosphotyrosine mAb PY20 (Transduction Laboratories). The levels of IRS-1, IGF-IR, SHC expression were determined by stripping the phosphotyrosine blots and reprobing them with the following Abs: for IRS-1: anti-IRS-1 pAb (UBI); for IGF-IR: anti-IGF-IR mAb (Santa Cruz); for SHC: anti-SHC mAb (Transduction Laboratories). The association of GRB2 or p85 with IRS-1 or SHC was visualized in IRS-1 or SHC blots using an anti-GRB2 mAb (Transduction Laboratories) or an anti-p85 mAb (UBI), respectively. The intensity of bands was measured by laser densitometry scanning.

Northern Blotting. The levels of IRS-1 mRNA were detected by Northern blotting in 20 ug of total RNA using a 631 bp probe derived from a mouse IRS-1 cDNA (nt 1351-2002). This fragment (99.8% homology with the human IRS-1 sequence) hybridizes with both human and mouse IRS-1 mRNA (31, 32).

Statistical Analysis. The results in cell growth experiments were analyzed by ANOVA or Student t-test, where appropriate.

RESULTS

ICI 182,780 inhibits the growth of MCF-7 cells with amplified IGF-IR signaling. Sensitivity to ICI 182,780 is determined by the cellular levels of IRS-1. All cell lines used in this study secrete autocrine IGF-I-like mitogens and are able to proliferate in PRF-SFM (15, 17, 21). The basal (autocrine) growth of the cells was enhanced in the presence of IGF-I (Fig. 1A and B). Short (1-2 days) treatments with ICI 182,780 were not sufficient to inhibit cell growth (data not shown), but a 4-day culture in the presence of the antiestrogen produced evident cytostatic effects (Fig. 1A and B). In general, the response to ICI 182,780 was dose-dependent (Fig. 1A and B), however, compared with the other cell lines, the cells highly overexpressing IRS-1(MCF-7/IRS-1 clones 3 and 18) were more resistant to the drug (Fig. 1B and C). Specifically, 1 nM ICI

182,780 inhibited the basal growth by 80, 55, and 50% in MCF-7, MCF-7/IGF-IR, and MCF-7/SHC cells, respectively, but the same dose produced only a 20-30% growth inhibition in MCF-7/IRS-1, clones 3 and 18 (Fig. 1A and B). Higher concentrations of ICI 182,780 (10 and 100 nM) effectively suppressed the autocrine growth, or even induced cell death in all cell lines, except MCF-7/IRS-1, clone 18, where the maximal reduction (32%) of the basal growth occurred with a 100 nM dose (Fig. 1B).

In the presence of IGF-I, the effects of ICI 182,780 were attenuated. 1 nM ICI 182,780 was never cytostatic (data not shown), while 10 nM and 100 nM doses inhibited (by 30-50 % and 47-78%, respectively) IGF-I-dependent proliferation of cells with low IRS-1 levels (Fig. 1A and B). The same doses, however, were less efficient in MCF-7/IRS-1, clones 3 and 18, where growth reduction was 20-25% for 10 nM and 41-47% for 100 nM. Similarly, 300 nM ICI 182,780 produced a prominent cytostatic effect in all cell lines with low IRS-1 expression, but was less active in the clones highly overexpressing IRS-1 (70-93% versus 45-60% growth inhibition) (Fig. 1A, B and C).

The above results suggested that IRS-1 may be an important target for ICI 182,780 action. Consequently, in the next set of experiments we studied the effects of ICI 182,780 on the expression and function of IRS-1.

ICI 182,780 reduces IRS-1 levels and impairs IRS-1 signaling in MCF-7/IRS-1, MCF-7 and MCF-7/IGF-IR cells. In MCF-7/IRS-1 cells grown under basal conditions, IRS-1 was tyrosine phosphorylated for up to 4 days (Fig. 2A). IGF-I induced a rapid and marked (5-fold) increase of IRS-1 phosphorylation that persisted for up to 1 day and declined thereafter reaching close to the basal phosphorylation status at day 4. A short (≤ 1 day) treatment with ICI 182,780 had no consequences on IRS-1 expression or tyrosine phosphorylation. (Fig. 2A, panels a and b). However, p85/IRS-1 association was ~30% reduced under the basal conditions at day 1 of the treatment (Fig. 2A panel c).

The evident effect of ICI 182,780 action on IRS-1 expression and signaling occurred at day 4-day, and was especially pronounced in the absence of IGF-I. Specifically, without IGF-I, the drug suppressed IRS-1 protein expression by 60%, which was paralleled by a 60% reduction of IRS-1 tyrosine phosphorylation, and coincided with an almost complete (~95%) inhibition of p85/IRS-1 and GRB2/IRS-1 binding. The addition of IGF attenuated ICI 182,780 action, however, the effects of the treatment were still well detectable: IRS-1 levels were downregulated by 30%, IRS-1 tyrosine phosphorylation by 20%, p85/IRS-1 binding by 30%. Under IGF-I conditions, GRB2/IRS-1 binding was not appreciably affected (Fig. 2A, panels a-d).

Importantly, analogous action of ICI 182,780 on IRS-1 expression and tyrosine phosphorylation was seen in other studied cell lines (Fig. 2B). In both MCF-7/IGF-IR and MCF-7 cells containing only endogenous IRS-1, ICI 182,780 inhibited the IRS-1 expression under basal conditions by ~60%, which was paralleled by the reduced IRS-1 tyrosine phosphorylation (by ~90-95%). In the presence of IGF-I, the antiestrogen suppressed the IRS-1 levels by ~50% and IRS-1 tyrosine phosphorylation by ~40%.

ICI 182,780 attenuates IRS-1 mRNA expression. ICI 182,780 reduced the levels of ~5 kb IRS-1 mRNA (31) in MCF-7 and MCF-7/IGF-IR cells in the absence or presence of IGF-I, by 50 and 70%, respectively (Fig. 3). Moreover, the 5 kb message transcribed from the CMV-IRS-1 plasmid was downregulated (by ~70%) in MCF-7/IRS-1 cells treated with both IGF-I and ICI 182,780 (data not shown).

ICI 182,780 inhibits IGF-I-induced but not basal tyrosine phosphorylation of the IGF-IR. In MCF-7/IGF-IR cells, IGF-I moderately increased the expression of the IGF-IR. This effect was slightly (by 20%) blocked in the presence of ICI 182,780. Under the same conditions, the drug significantly (by 80%) reduced tyrosine phosphorylation of the IGF-IR (Fig. 4). ICI 182,780 had no effect on the basal expression of the IGF-IR, however, it produced a 30% increase in the basal tyrosine phosphorylation of the IGF-IR (Fig. 4). The latter peculiar effect of the antiestrogen occurred in several

repeat experiments. Short treatments with ICI 182,780 (≤ 1 day) were not associated with any significant changes in IGF-IR expression (data not shown).

Long-term ICI 182,780 treatment does not affect SHC signaling. In the presence of IGF-I, SHC tyrosine phosphorylation was moderately induced, with the maximum seen at 1 h upon stimulation. On the other hand, GRB2/SHC binding peaked at 15 min after IGF-I addition and declined thereafter with the minimal binding found at day 4 (Fig. 5). ICI 182,780 treatment, in the presence or absence of IGF-I, failed to induce significant changes in the levels or tyrosine phosphorylation of SHC proteins, except a transient stimulation of the basal SHC tyrosine phosphorylation at 15 min (Fig. 5). Importantly, at all time points, SHC/GRB2 association was not influenced by the drug.

Interestingly, at day 4, SHC tyrosine phosphorylation and SHC/GRB2 binding were suppressed in the presence of IGF-I (Fig. 5). This characteristic regulation of SHC by IGF-I, documented by us previously in MCF-7 cells and MCF-7-derived clones, was not affected by ICI 182,780 (29).

Similar lack of ICI 182,780 effects on SHC expression and signaling was noted in MCF-7 and MCF-7/IGF-IR cells (data not shown).

DISCUSSION

Pure antiestrogens have been shown to interfere with one of the most important systems regulating the biology of hormone-dependent breast cancer cells, namely the IGF-I system (1, 3, 6, 18, 19, 33-35). The compounds inhibit IGF-induced proliferation, which is associated with such phenomena as downregulation of IGF binding sites and reduction of IGF availability (3, 18, 19). Similar action has been ascribed to non-steroidal antiestrogens such as Tam or 4-OH-Tam (4).

The effects of pure antiestrogens on the IGF signal transduction have been unknown. Here, we studied if and how ICI 182,780 modulates the IGF-IR intracellular pathways in breast cancer cells. We focused on the relationship between drug efficiency

and signaling capacities of the IGF-IR or IRS-1 since these molecules appear to control proliferation and survival in breast cancer cells (11, 12, 21, 25, 26, 36).

Previously we found that cytostatic action of Tam involves its interference with IGF signaling pathways. In particular, Tam suppressed tyrosine phosphorylation of IRS-1 and caused hyperphosphorylation of SHC (29). The most important conclusion of the present work is that inhibition of IRS-1 expression is an important element of ICI 182,780 mode of action. The first observation was that amplification of IGF signaling did not abrogate sensitivity to ICI 182,780. Next, ICI 182,780 appeared to affect a specific IGF signaling pathway, as the efficiency of the drug was dictated by the cellular levels of IRS-1, but not that of SHC or the IGF-IR. For instance, MCF-7/IGF-IR clone 17 was very sensitive to ICI 182,780 despite a 12-fold IGF-IR overexpression, whereas MCF-7/IRS-1, clones 3 and 18 (7 and 9-fold IRS-1 overexpression, respectively) were quite resistant to the drug (15, and Fig. 1). Moreover, ICI 182,780 reduced IRS-1 levels and tyrosine phosphorylation in several cell lines in the presence or absence of IGF-I, while its action on the IGF-IR was limited to the inhibition of IGF-I-induced tyrosine phosphorylation, and its effects on SHC were none.

The reduction of IRS-1 expression by ICI 182,780 occurred in all studied cell lines, however it was clearly more pronounced in the cells expressing low levels of the substrate (Fig. 2). This suggests that downregulation of IRS-1 by ICI 182,780 is a saturable process and overexpression of IRS-1 may provide resistance to the drug. Indeed, although we did not notice a strict correlation between IRS-1 levels or IRS-1 tyrosine phosphorylation and ICI 182,780-dependent growth inhibition, IRS-1 overexpressing cells tended to be more resistant to the cytostatic action of the antiestrogen (Fig. 1). Interestingly, overexpression of IRS-1 clearly had a greater impact on the response to high doses of ICI 182,780 (≥ 100 nM) than on the effects of low drug concentrations. This could suggest that ICI 182,780 action is multiphased, with the initial inhibition being IRS-1-independent (but perhaps, ER-

dependent) and the strong growth reduction associated with the blockade of IRS-1 function (Fig. 1 and 2).

ICI 182,780 affected IRS-1 expression not only on the level of protein but also on the level of mRNA. In our experiments, the antiestrogen reduced the expression of IRS-1 mRNA in the presence or absence of IGF-I. However, the mechanism by which ICI 182,780 interferes with IRS-1 mRNA expression was not studied here and it remains speculative. Regarding transcriptional regulation, no estrogen responsive elements have been mapped in the IRS-1 promoter, but it can not be ruled out that ICI 182,780 acts indirectly through some other regulatory sequences in the 5' untranslated region of IRS-1 gene, such as AP1, AP2, Sp1, C/EBP, E box (37, 38). A postranscriptional component may be argued by the fact that the inhibition of IRS-1 mRNA by ICI 182,780 was evident in IGF-I-treated MCF-7/IRS-1 cells, in which the majority of IRS-1 message originated from the expression plasmid devoid of any IRS-1 promoter sequences (CMV-driven IRS-1 cDNA)(39) (data not shown). In addition, the finding that ICI 182,780 similarly inhibited IRS-1 mRNA levels under the basal and IGF-I conditions, but IRS-1 protein was significantly more reduced in the absence of IGF-I (Fig. 3 vs. Fig. 2 A) could suggest that the drug acts upon some IGF-I-dependent mechanism controlling mRNA stability, translation, or posttranslational events. In fact, in other experimental systems, IGF-I or insulin regulated various messages, including IRS-1 mRNA, on the postranscriptional level (38, 40, 41).

In its action on IRS-1, ICI 182,780 appeared more potent than Tam which decreased tyrosine phosphorylation of IRS-1 but did not cause any detectable changes in IRS-1 expression. Our results with Tam suggested that this antiestrogen may influence the activity of tyrosine phosphatases (29). An interaction with the phosphatase system has also been suggested for pure antiestrogens (42). In the present work, ICI 182,780 effects on phosphatases acting on IRS-1 were impossible to assess, since the drug affected also IRS-1 expression (Fig. 3). However, some interference of ICI 182,780 with the

phosphorylation/dephosphorylation events could be indicated for instance by our experiments with the IGF-IR, where the compound induced IGF-IR phosphorylation under the basal conditions and IGF-IR dephosphorylation in the presence of IGF-I, without evident modifications of the receptor expression (Fig. 4).

Other important observations stemming from this work concern similarities and differences between the effects of ICI 182,780 and Tam on the IGF-IR and SHC. While Tam did not modulate the expression of IGF-IR protein (29), ICI 182,780 moderately decreased IGF-IR levels in the presence of IGF-I. The action of ICI 182,780 and Tam on IGF-IR tyrosine phosphorylation was similar, namely, both compounds inhibited IGF-I-induced but not basal tyrosine phosphorylation of the IGF-IR. The effects of ICI 182,780 and Tam on SHC were different. With Tam, we observed elevated tyrosine phosphorylation of SHC proteins and increased SHC/GRB2 binding in growth arrested cells, while ICI 182,780 did not affect SHC phosphorylation or expression (29). Thus, induction of a non-mitogenic SHC signaling is a peculiarity of Tam but not ICI 182,780 mechanism of action.

In summary, cytostatic effects of ICI 182,780, similar to Tam, are associated with the inhibition of IGF-IR signaling. The mitogenic/survival IRS-1 pathway is a target for both antiestrogens. Both drugs reduce the levels of tyrosine phosphorylated IRS-1, but only ICI 182,780 clearly inhibits expression of the substrate. High cellular levels of IRS-1 hinder the response to higher doses of ICI 182,780, thus overexpression of IRS-1 in breast tumors may represent an important mechanism of antiestrogen resistance.

ACKNOWLEDGMENTS

This work was supported by the following grants and awards: NIH DK 48969 (E.S.); U.S. Department of Defense DAMD17-96-1-6250 (E.S.) and DAMD 17-97-1-7211 (M.A.G.); NCR Italy fellowships (D.S and M.S.).

ICI 182,780 used in this project was generously provided by Dr. A. Wakeling, ZENECA, Great Britain.

REFERENCES

1. Wakeling, A. E., Dukes, M., and Bowler, J. (1991) *Cancer Res.* **51**, 3867-3873.
2. Robertson, J. F. R., Howell, A., DeFriend, D. J., Blamey, R. W., and Walton, P. (1997) *Breast* **6**, 186-189.
3. de Cupis, A., and Favoni, R. E. (1997) *Trends in Pharmacol. Sci.* **18**, 245-251.
4. Chander, S. K., Sahota, S. S., Evans, T. R. J., and Luqmani, Y. A. (1993) *Crit. Rev. Oncol. Hematol.* **15**, 243-269.
5. Osborne, C. K., Coronado-Heinsohn, E. B., Hilsenbeck, S. G., McCue, B. L., Wakeling, A. E., McClelland, R. A., Manning, D. L., and Nickolson, R. I. (1995) *J. Natl. Cancer Inst.* **87**, 746-750.
6. de Cupis, A., Noonan, D., Pirani, P., Ferrera, A., Clerico, L., and Favoni, R. E. (1995) *Br. J. Pharm.* **116**, 2391-2400.
7. Nicholson, R. I., Gee, J. M., Manning, D. L., Wakeling, A. E., Montano, M. M., and Katzenellenbogen, B. S. (1995) *Ann. NY Acad. Sci.* **761**, 148-163.
8. Pavlik, E. J., Nelson, K., Srinivasan, S., Depriest, P. D., and Kenady, D. E. (1996) in *Estrogens, Progestins, and their Antagonists* (Pavlik, E. J., Ed.) pp. 116-159, Vol. 1, Birkhauser, Boston.
9. Larsen, S. S., Madsen, M. W., Jensen, B. L., and Lykkesfeld, A. E. (1997) *Int. J. Cancer* **72**, 1129-1136.
10. Wiseman, L. R., Johnson, M. D., Wakeling, A. E., Lykkesfeldt, A. E., May, F. E., and Westley, B. R. (1993) *Eur. J. Cancer* **29A**, 2256-2264.
11. Lee, A. V., and Yee, D. (1995) *Biomed. Pharmacother.* **49**, 415-421.
12. Surmacz, E., Guvakova, M. A., Nolan, M. K., Nicosia, R., and Sciacca, L. (1998) *Breast Cancer Res. Treat.* **47**, 255-267.
13. Dickson, R. B., and Lippman, M. E. *Endocrin. Rev.* (1995) **16**, 559-589.
14. Doerr, M., and Jones, J. (1996) *J. Biol. Chem.* **271**, 2443-2447.
15. Guvakova, M. A., and Surmacz, E. (1997) *Exp. Cell. Res.* **231**, 149-162.
16. Bracke, M. E., Vyncke, B. M., Bruyneel, E. A., Vermeulen, S. J., De Bruyne, G. K., Van Larebeke, N. A., Vleminck, K., Van Roy, F. M., and Mareel, M. M. (1993) *Br. J. Cancer* **68**, 282-289.
17. Nolan, M. K., Jankowska, L., Prisco, M., Xu, S., Guvakova, M., and Surmacz, E. (1997) *Int. J. Cancer* **72**, 828-833.
18. Hung, H., and Pollak, M. (1995) *Prog. Growth Factor Res.* **6**, 495-501.
19. Huynh, H., Yang, X. F., and Pollak, M. (1996) *Cell Growth Different.* **7**, 1501-1506.

20. Cullen, K.J., Lippman, M.E., Chow, D., Hill, S., Rosen, N., and Zwiebel, J.A. (1992) *Mol. Endocrinol.* **6**, 91-100.
21. Surmacz, E., and Burgaud, J-L. (1995) *Clin. Cancer Res.* **1**, 1429-1436.
22. Peyrat, J.P., and Bonnetterre, J. (1992) *Breast Cancer Res. Treat.* **22**, 59-68.
23. Papa, V., Gliozzo, B., Clark, G. M., McGuire, W. L., Moore, D., Fujita-Yamaguchi, Y., Vigneri, R., Goldfine, and I. D., Pezzino, V. (1993) *Cancer Res.* **53**, 3735-3740.
24. Resnik, J. L., Reichart, D. B., Huey, K., Webster, N. J. G., Seely, B. L. (1998) *Cancer Res.* **58**, 1159-1164.
25. Rocha, R. L., Hilsenbeck, S. G., Jackson, J. G., and Yee, D. (1997) *Clin. Cancer Res.* **3**, 103-109.
26. Turner, B. C., Haffty, B. G., Nayarannan, L., Yuan, J., Havre, P. A., Gumbs, A., Kaplan, L., Burgaud, J-L., Carter, D., Baserga, R., and Glazer, P. (1997) *Cancer Res.* **57**, 3079-3083.
27. Ellis, M. J. C., Singer, C., Hornby, A., Rasmussen, A., and Cullen, K. J. (1994) *Breast Cancer Res. Treat.* **31**, 249-261.
28. Hankinson, S., Willet, W. C., Colditz, G., Hunter, D. J., Michaud, D. S., Deroo, B., Rosner, B., Speizer, F., and Pollak, M. (1998) *Lancet* **351**, 1393-1396.
29. Guvakova, M. A., and Surmacz, E. (1997) *Cancer Res.* **57**, 2606-2610.
30. Sepp-Lorenzino, L. (1998) *Breast Cancer Res. Treat.* **47**, 235-253.
31. Nishiyama, M., and Wands, J. R. (1992) *Bioch. Biophys. Res. Comm.* **183**, 280-285.
32. Keller, S. R., Aebersold, R., Garner, C. W., and Lienhard, G. E. (1993) *Bioch. Biophys. Acta* **1172**, 323-326.
33. Nicholson, R. I., Gee, J. M., Bryant, S., Francis, A. B., McClelland, R. A., Knowlden, J., Wakeling, A. E., and Osborne, C. K. (1996) *Ann. NY Acad. Sci.* **784**, 325-335.
34. Wakeling, A. E., Newbould, E., and Peters, S. W. (1989) *J. Mol. Endocrin.* **2**, 225-234.
35. Coradini, D., Biffi, A., Cappelletti, V., and Di Fronzo, G. (1994) *Anticancer Res.* **14**, 1059-1064.
36. Dunn, S. E., Hardman, R. A., Kari, F. W., and Barrett, J. C. (1997) *Cancer Res.* **57**, 2687-2693.
37. Matsuda, K., Araki, E., Yoshimura, R., Tsuruzoe, K., Furukawa, N., Kaneko, K., Motoshima, H., Yoshizato, K., Kishikawa, K., and Shichiri, M. (1997) *Diabetes* **46**, 354-362.

38. Araki, E., Haag, B. L., Matsuda, K., Shichiri, M., and Kahn, C. R. (1995) *Mol. Endocrin.* **9**, 1367-1379.
39. D'Ambrosio, C., Keller, S. R., Morrione, A., Lienhard, G. E., Baserga, R., and Surmacz, E. (1995) *Cell Growth Different.* **6**, 557-562.
40. Miura, M., Li, S-W., Dumenil, G., and Baserga, R. (1994) *Cancer Res.* **54**, 2472-2477.
41. Lee, A. V., Weng, C-N., Jackson, J. G., and Yee, D. (1997) *J. Endocrin.* **152**, 39-47.
42. Freiss, G., and Vignon, F. (1994) *Mol. Endocrinol.* **8**, 1389-1396.

FOOTNOTES

¹Corresponding author, at Kimmel Cancer Center, Thomas Jefferson University,
233 S. 10th Street, Philadelphia, PA 19107, Fax: 215-923-0249
e-mail: surmacz1@jeflin.tju.edu

²The abbreviations used are: CS, calf serum; ER, estrogen receptor; E2, 17-beta estradiol; GRB2, growth factor receptor-bound protein 2; IGF-I, insulin-like growth factor I; IGF-IR, IGF-I receptor; IGFBP, IGF binding protein; IP, immunoprecipitation; IRS-1, insulin receptor substrate 1; MCF-7/IGF-IR, MCF-7 cells overexpressing IGF-IRs; MCF-7/IRS-1, MCF-7 cells overexpressing IRS-1; MCF-7/SHC, MCF-7 cells overexpressing SHC; PI-3 kinase, phosphatidylinositol 3 kinase; PRF-SFM, phenol red-free serum-free medium; SHC, src/collagen homology proteins; Tam, Tamoxifen; 4-OH-Tam, 4-hydroxytamoxifen; WB, Western immunoblotting.

³Sisci, D., Mauro, L., Salerno, M., Kim, J., Tam, T., Guvakova, M., Ando, S., and Surmacz, E. "Role of SHC in adhesion and motility in breast cancer cells", submitted.

FIGURE LEGENDS

Fig. 1. ICI 182,780 inhibits the growth of MCF-7 cells overexpressing different elements of IGF-IR signaling. IRS-1 levels determine ICI 182,780 sensitivity. A) ICI 182,780-induced growth inhibition in the parental MCF-7 cells (8×10^4 IGF-IRs/cell), MCF-7/IGF-IR, clone 17 (1×10^6 IGF-IRs/cell), MCF-7/SHC (5-fold SHC overexpression over the level in MCF-7 cells). B) Growth reduction in MCF-7/IRS-1 clone 9 (3-fold IRS-1 overexpression over the levels in MCF-7 cells), clone 3 (7-fold overexpression), and clone 18 (9-fold overexpression). The cells were treated with different doses of ICI 182,780 in the presence or absence of 50 ng/ml IGF-I, as described under Materials and Methods. The increase in cell number between day 0 and day 4 is taken as 100%. The results are means from at least 4 experiments. Bar, SE. C) Levels of IRS-1 protein in different MCF-7/IRS-1 cell lines. IRS-1 levels were determined by immunoprecipitation and Western blotting as described under Materials and Methods. Representative results from 3 experiments are shown.

Fig. 2. ICI 182,780 inhibits IRS-1-mediated signaling. A) Effects of ICI 182,780 in MCF-7/IRS-1, clone 3. IRS-1 tyrosine phosphorylation (IRS-1 PY) (panel a), protein levels (IRS-1) (panel b) as well as IRS-1-associated p85 of PI-3 kinase (panel c) and GRB2 (panel d) were determined in cells treated for 15 min, 1h, 1 day or 4 days with 100 nM ICI 182,780 in the presence or absence of 50 ng/ml IGF-I. In 1h treatment, the lane IGF(-) ICI (-) is underloaded. Representative results from 5 experiments are shown. B) Effects of ICI 182,780 on IRS-1 in MCF-7/IGF-IR and MCF-7 cells. IRS-1 tyrosine phosphorylation (IRS-1 PY) and protein levels (IRS-1) were examined in cells treated with 100 nM ICI 182,780 for 4 days. Representative blots of 5 experiments are shown.

Fig. 3. ICI 182,780 attenuates the expression of IRS-1 mRNA. IRS-1 mRNA levels in MCF-7 and MCF-7/IGF-IR cells. The expression of IRS-1 mRNA was determined in cells treated with 100 nM ICI 182,780 for 4 days in the presence or absence of IGF-I. Panel a, IRS-1 mRNA ~5 kb; panel b, control RNA loading: 28S and 18 S RNA in the same blot.

Fig. 4. Effects of ICI 182,780 on the IGF-IR. IGF-IR tyrosine phosphorylation (IGF-IR PY) and protein levels (IGF-IR) in MCF-7/IGF-IR, clone 17 treated for 4 days with 100 nM ICI 182,780 in the presence or absence of 50 ng/ml IGF-I. Representative results of 3 different experiments are shown.

Fig. 5. Effects of ICI 182,780 on SHC signaling. SHC tyrosine phosphorylation (SHC PY), protein levels (SHC), and SHC-associated GRB2 were studied in MCF-7/SHC cells treated for 4 days with 100 nM ICI 182,780 in the presence or absence of 50 ng/ml IGF-I. Representative results of 5 experiments are shown.

Figure 1A

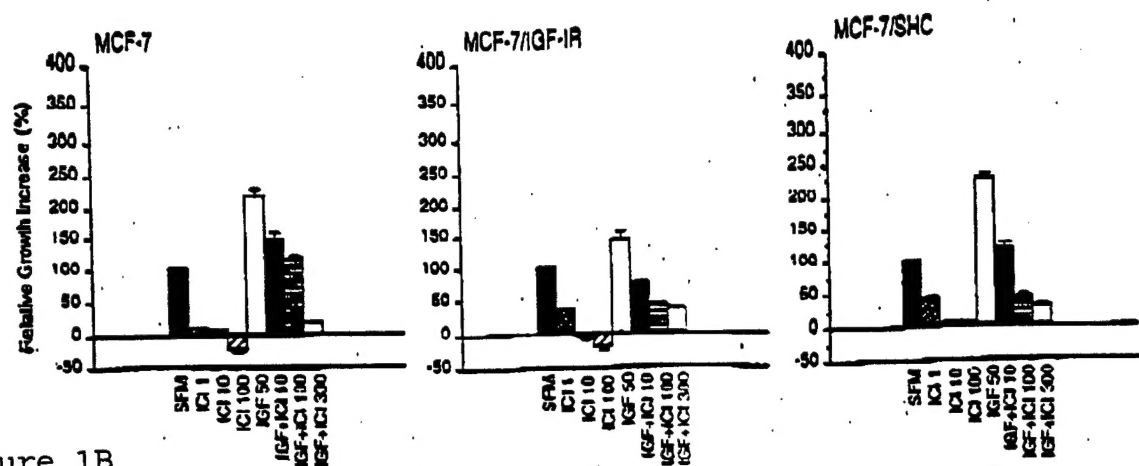


Figure 1B

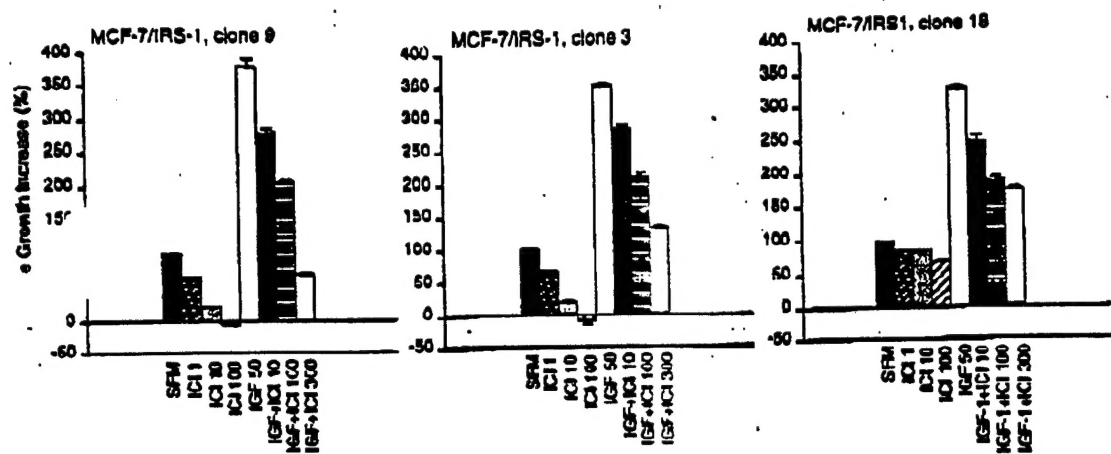


Figure 1C

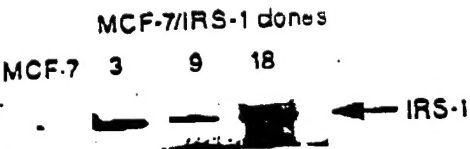


Figure 2A

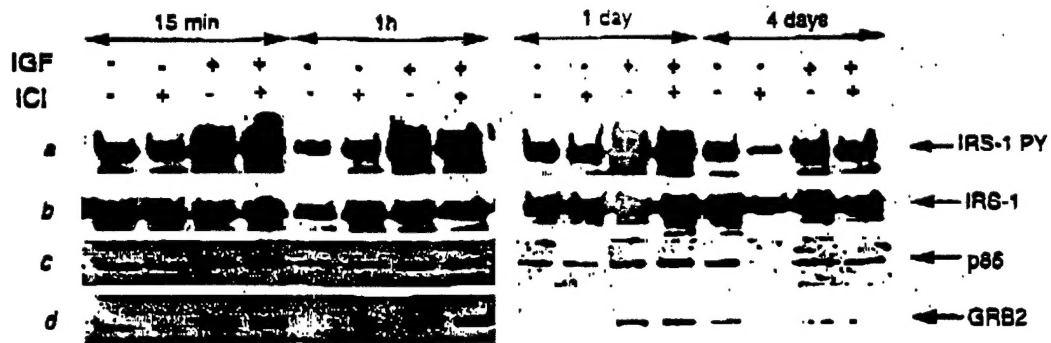


Figure 2B

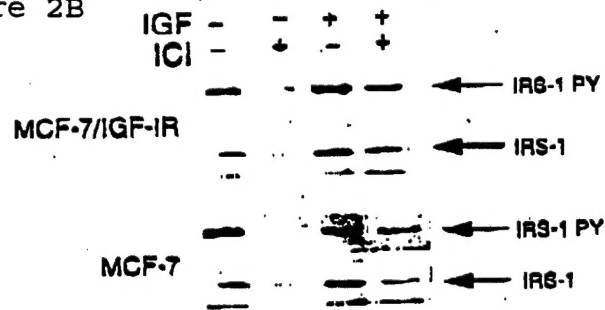


Figure 3

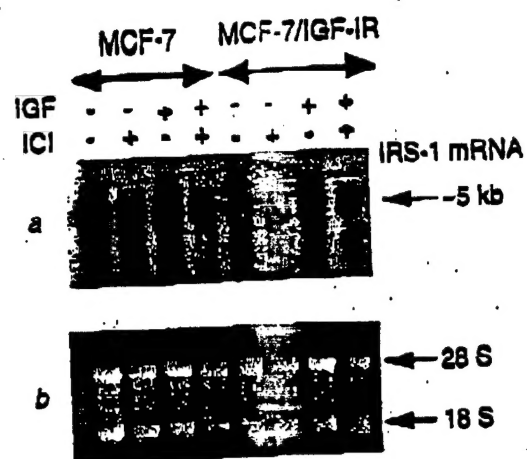


Figure 4

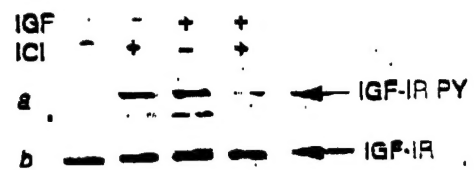


Figure 5

